universität wien

DIPLOMARBEIT / DIPLOMA THESIS

Titel der Diplomarbeit / Title of the Diploma Thesis

„Role of sphingosine kinase 1 expression in the osteoblast-osteoclast crosstalk“

verfasst von / submitted by

Lisa-Maria WINKLER

angestrebter akademischer Grad / in partial fulfilment of the requirements for the degree of

Magistra der Pharmazie (Mag.pharm.)

Wien, 2018 / Vienna, 2018

Studienkennzahl lt. Studienblatt / degree programme code as it appears on the student record sheet:	A 449
Studienrichtung lt. Studienblatt / degree programme as it appears on the student record sheet:	Diplomstudium Pharmazie
Betreut von / Supervisor:	ao. Univ.-Prof. Mag. Dr. Oskar HOFFMANN

Eidesstattliche Erklärung

Ich erkläre hiermit an Eides statt, dass ich die vorliegende Arbeit selbstständig und ohne Benutzung anderer als der angegebenen Hilfsmittel angefertigt habe. Die aus fremden Quellen direkt oder indirekt übernommenen Gedanken sind als solche kenntlich gemacht.

Die Arbeit wurde bisher in gleicher oder ähnlicher Form keiner anderen Prüfungsbehörde vorgelegt und auch noch nicht veröffentlicht.

Danksagung

An dieser Stelle möchte ich mich bei allen für die Unterstützung während meines Studiums und vor allem während der Arbeit an meiner Diplomarbeit bedanken.

Zuerst bedanke ich mich bei Herrn Dr. Hoffmann, der es mir ermöglicht hat, wissenschaftlich zu forschen und in das Forscherleben einzutauchen. Ebenso danke ich Frau Mag.ª Kampleitner, deren Hilfsbereitschaft und Motivation unerschöpflich waren. Dank gebührt auch Frau Berger und Herrn Höflich, die mir geduldig die professionelle Arbeitsweise im Labor gezeigt haben. Nicht zuletzt danke ich auch meinen Mitstudentinnen für den regen Austausch.

Besonders danken möchte ich auch meiner Familie und meinen Freundinnen und Freunden für die Unterstützung während des Studiums und die oftmals notwendige Abwechslung vom Studienalltag.

Ein spezielles Danke auch an meinen Mann, der immer für mich da ist und mich motiviert und bestärkt in dem, was mir wichtig ist.

Abbreviations used:

ALP	alkaline phosphatase
APS	ammonium persulfate
BM	bone marrow
BMP6	bone morphogenetic factor 6
BMM	bone marrow-derived macrophages
BSA	bovine serum albumin
CC	osteoblast-osteoclast co-culture
EDG	endothelial differentiation gene
EDTA	ethylenediaminetetraacetic acid
ERK	extracellular signal-regulated kinases
FCS	fetal calf serum
HI	heat inactivated
HRP	horseradish peroxidase
IGF1	insulin-like growth factor 1
IgG	immunoglobulin G
M-CSF	macrophage colony stimulating factor
MEM	minimal essential medium
OB	osteoblast
OC	osteoclast
OPG	osteoprotegerine
PBS	phosphate buffered saline
PMSF	phenylmethylsulphonyl fluoride

RANKL	receptor activator of nuclear factor kappa B ligand
RBC	red blood cell
rh	recombinant human
RIPA	radioimmunoprecipitation assay buffer
rm	recombinant mouse
RT-PCR	real time - polymerase chain reaction
Runx2	runt-related transcription factor 2
S1P	sphingosine-1-phosphate
SDS	sodium dodecyl sulfate
SphK	sphingosine kinase
Spns2	sphingolipid transporter 2
TBS	Tris-buffered saline
TRAF2	TNF receptor-associated factor 2
TRAP	tartrate resistant acid phosphatase
Tris	Tris (hydroxymethyl) aminomethane
TNFα	tumour necrosis factor alpha
Wnt10b	wingless-related integration site 10b

Table of contents

1. Aim of the thesis

Cells can react to their environment and communicate with neighboring cells via soluble signaling molecules, cytokines. In bone the two main cell types are osteoclasts, which break down existing bone matrix, and osteoblasts, which are rebuilding the structures. From osteoblasts two other cell types can evolve: Bone lining cells, which are mostly inactive and serve as a protective layer on the finished bone matrix, and osteocytes, which are embedded in the matrix and can sense mechanical stimulations. It is widely known that the secretion of M-CSF and RANKL from osteoblasts is imperative for osteoclastogenesis. The secretory role of osteoclasts, especially non-resorbing osteoclasts, is being investigated. Cytokines secreted by those cells are also called clastokines; they seem to have a stimulatory effect on osteoblast mineralization.

To study clastokines we first had to establish a reliable cell-derived osteoclast culture model supplemented with M-CSF and RANKL. The culture should grow over four to five days during which we chose three time points representing the stages of osteoclastogenesis. First the undifferentiated cells, then the osteoclast precursor and finally the multinucleated, mature osteoclasts.

Figure 1: Overview of osteoclastogenesis

We chose to research sphingosine kinase 1, the enzyme that is responsible for transforming sphingosine into sphingosine-1-phosphate. In several papers (Ishii, et al. 2010, Pederson, et al. 2008, Ryu, et al. 2006) this kinase was shown to increase during the osteoclastogenesis. Sphingosine-1-phosphate is a ubiquitous signaling molecule that might also play an important role in osteoclast-osteoblast crosstalk.

2. Introduction

The skeleton accounts for about 18% of our body weight and is not only responsible for supporting the body but also has several other functions: protection of the inner organs, movement, mineral homeostasis of calcium and phosphate as well as blood cell production and storage of triglycerides in the bone cavities (Tortora and Derrickson 2008). In the last few years studies suggested that bone might also function as an endocrine organ, e.g. secreting osteocalcin (Guntur and Rosen 2012). The skeleton consists of different types of bone depending on the functionality needed. The long bones provide a hollow shaft in which haematopoiesis can occur, in contrast to the dense cortical bone that mainly provides protection, for example the skull. All types of bone consist of a modified form of hydroxyapatite ($Ca_{10}(PO_4)_6(OH)_2$) embedded in a collagen matrix (Albrecht and Hornbostel 1978). Bone growth continues throughout adulthood; the repair of micro cracks can occur spontaneously following physical exercise or mechanical stress (Seref-Ferlengez, et al. 2015).

There are four cell types specific for the bone: bone lining cells, osteocytes, osteoblasts and osteoclasts. Bone lining cells and osteocytes are further differentiated osteoblasts. In this work I intend to focus mainly on osteoclasts, the other cell types will be mentioned only briefly.

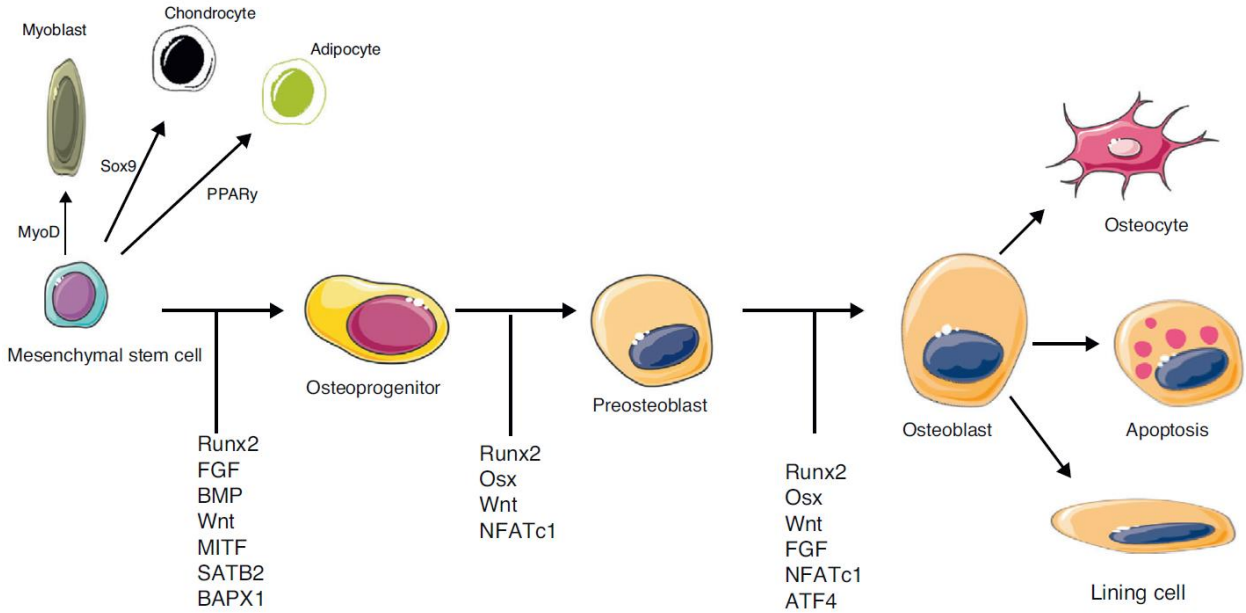

Figure 2: Overview of osteoblast differentiation and activation, as well as the molecular signals that play a key role. From Arboleya and Castañeda 2013.

Osteoblast precursors evolve from stromal mesenchymal stem cells. These cells can either differentiate into muscle cells, adipocytes, chondrocytes or osteoblasts, depending on the microenvironment they are exposed to (Grigoriadis 1988). The so-called 'master regulator' of osteoblast differentiation is the Runx2 gene (Arboleya and Castañeda 2013, Florencio-Silva, et al. 2015), which is imperative for osteoblast formation. Several other genes and cytokines play a role in the differentiation process, for example the bone morphogenetic proteins (Chen, et al. 2012). The main role of the mature osteoblast is the formation of bone matrix. First the cells create the organic matrix, which is made of collagenous proteins. Then the mineral matrix, consisting of hydroxyapatite crystals, is added. This process is supported by the secretion and action of alkaline phosphatase (ALP) is secreted, which is therefore considered to be an important osteoblast marker (Clarke 2008, Florencio-Silva, et al. 2015).

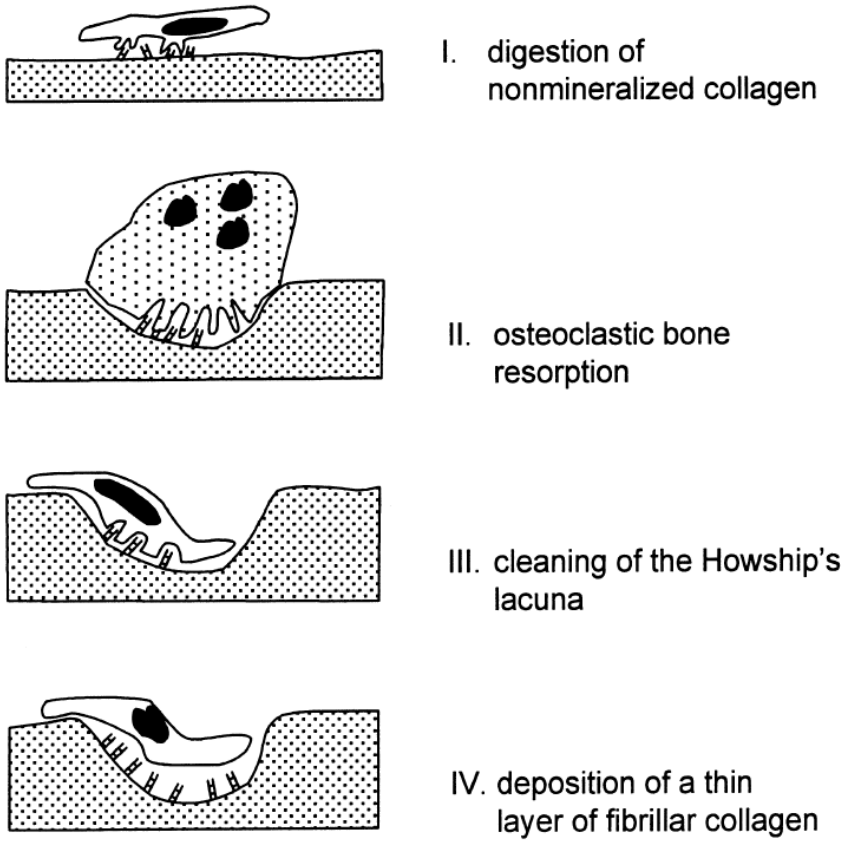

Figure 3: Schematic presentation of the events involved in the coupling of bone resorption and formation, as proposed by Everts, et al. 2002. Bone lining cells digest protruding collagen fibrils before osteoclasts attach to the surface. After the creation of the Howship's lacuna, the bone lining cells are again digesting protruding collagen fibrils and deposit a thin layer of collagen before osteoblasts start their mineralization process.

After the mineralization process osteoblasts can stay on the surface of the newly formed bone matrix and evolve further into bone lining cells. These are, in contrast to the actively mineralizing osteoblasts, flattened and have only sparse secretory granules as well as a moderate rough endoplasmic reticulum and Golgi system. Bone lining cells play an active role in the remodelling process by digesting nonmineralized collagen remnants and preparing the Howship lacunae for osteoclastic resorption or bone formation from osteoblasts (Everts, et al. 2002). They express typical osteoblast markers like ALP (Clarke 2008) and are connected with each other and also to osteocytes via gap junctions (Florencio-Silva, et al. 2015).

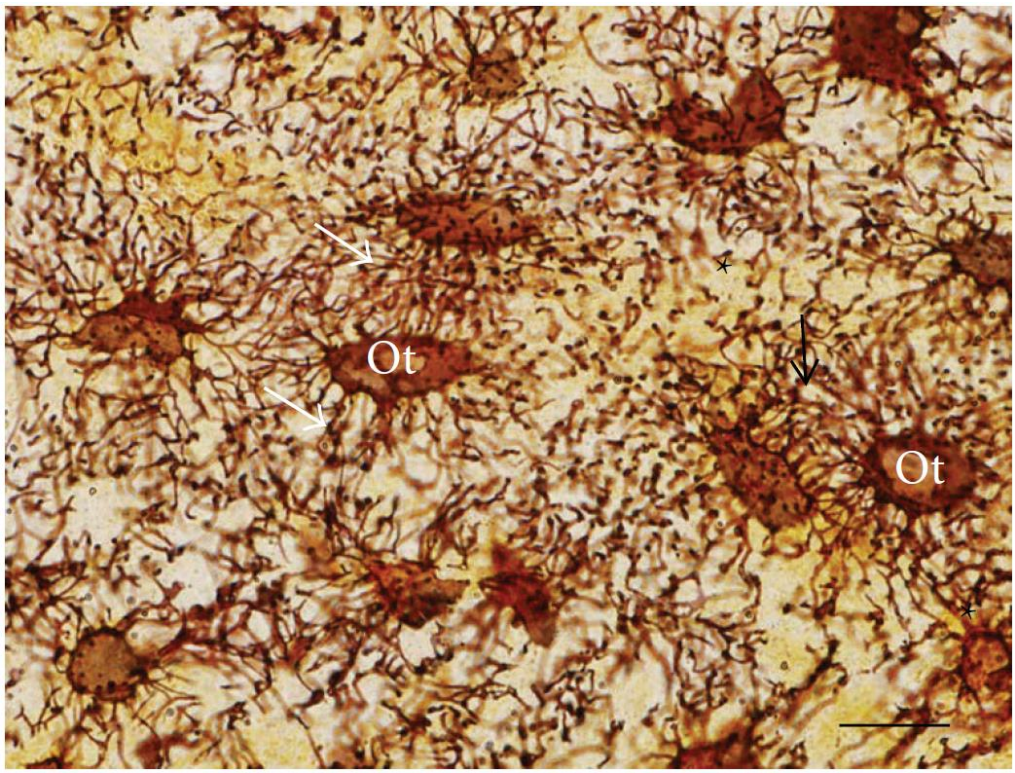

Figure 4: Light micrograph of alveolar bone from rats. Silver impregnation method shows osteocytes (Ot) connecting with each other (Florencio-Silva, et al. 2015).

During the mineralization process, approximately 10% of all mature osteoblasts become embedded in the newly formed bone matrix and evolve further into osteocytes. Using a system of tiny tunnels, called canaliculi, reaching from the lacuna space the osteocytes create a system to communicate and transmit a variety of signals, e.g. as response to mechanical stress or reduced gravitation. If the bone does not get remodelled, the osteocytes are able to live several years (Arboleya and Castañeda 2013, Bonewald 2011, Florencio-Silva, et al. 2015). Dying osteocytes secrete factors that induce osteoclast differentiation and activity (Kogianni, et al. 2008). This can be induced by a decrease in oestrogen or a glucocorticoid treatment and may thus lead to increased bone degradation (Clarke 2008). It is also suspected that osteocytes might have an endocrine role by secreting osteocalcin (Guntur and Rosen 2012).

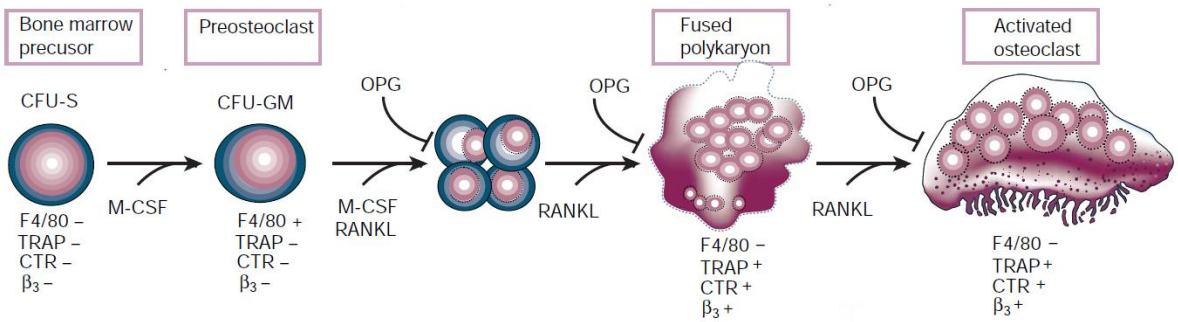

Figure 5: Schema of osteoclastogenesis, adapted from Boyle, et al. 2003. When the preosteoclasts evolve into a fused polycaryon they also become TRAP positive. Osteoprotegerin inhibits cell fusion and activation of osteoclasts.

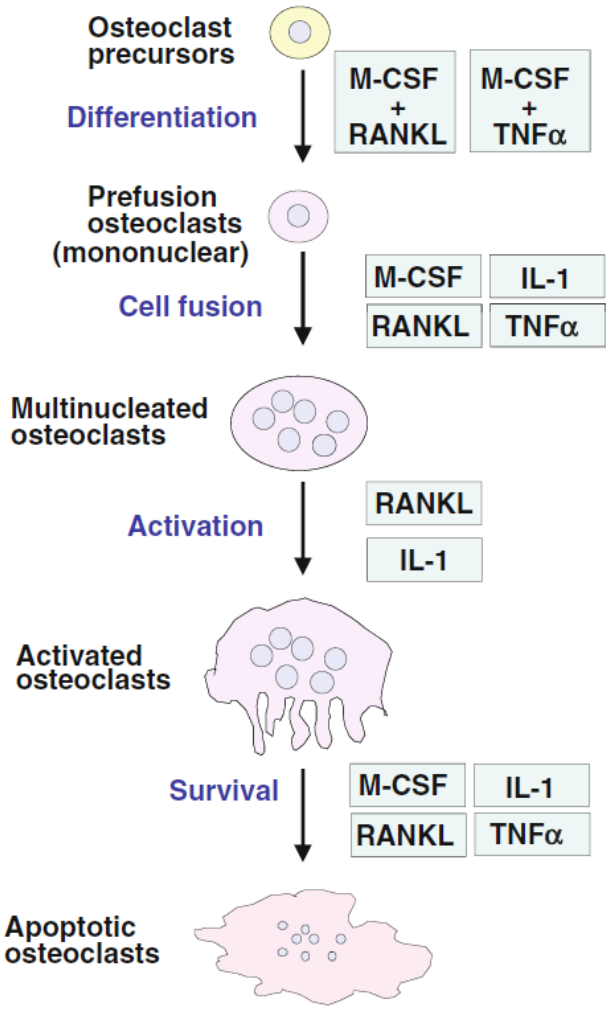

Figure 6: Osteoclast differentiation and function, schema from Nakamura, et al. 2012. At the different stages of osteoclast activation, different cytokines are involved. The presence of RANKL is required at all stages.

Precursor cells from the monocyte-macrophage haematopoietic lineage can develop into mature, multinucleated osteoclasts under the influence of several factors. To evolve into the preosteoclast, the presence of M-CSF (macrophage colony stimulating factor) is necessary. Further development into prefusion osteoclasts requires the presence of RANKL (receptor activator of NF- κB ligand) or TNFα. Continued influence of RANKL leads to fusion of precursor cells into multinucleated osteoclasts. When the osteoclast is activated it adheres to the bone matrix by forming a sealed zone by rearranging the actin into a ring. Inside this sealed zone the release of H^+ ions and Cl^- ions creates an acidic milieu in which the mineral matrix dissolves in concert with enzymes like cathepsin K and TRAP (tartrate resistant acid phosphatase). They are only active at an acidic pH and can digest the proteinaceous matrix (Boyle, et al. 2003, Clarke 2008, Florencio-Silva, et al. 2015, Nakamura, et al. 2012).

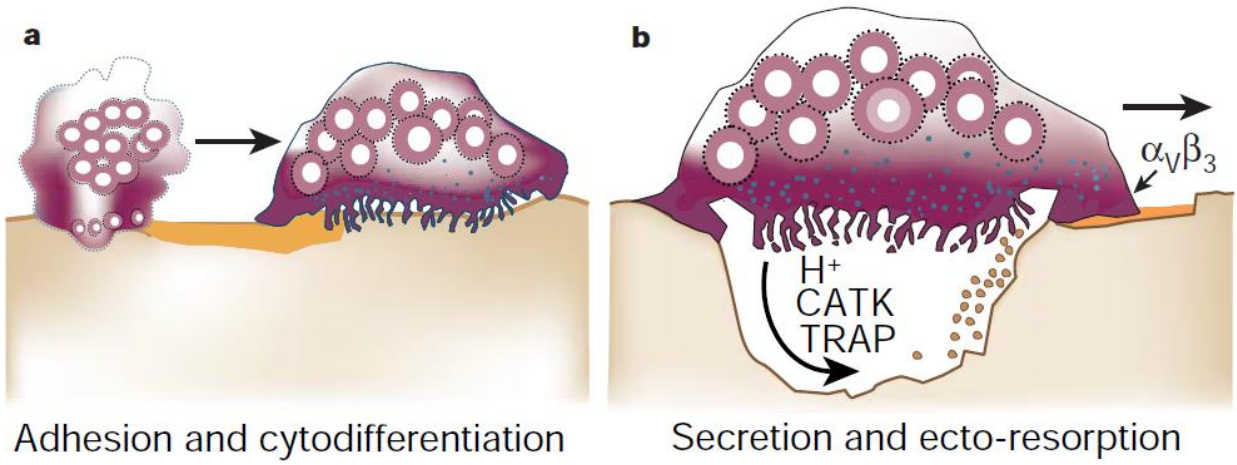

Figure 7: Activation of bone resorption from Boyle, et al. 2003. The fused polykaryons are moving towards the resorption site, where they adhere to the bone surface and undergo transformation into a mature osteoclast. The secretion of protons and lytic enzymes leads to degradation of the bone mineral and collagen matrices.

The main cell source of the cytokines needed for osteoclastogenesis are osteoblasts, as well as bone lining cells and osteocytes. All these cells are responsible for creating and maintaining a healthy skeleton. Bone needs to be rebuilt constantly, be it whether because of the need for Ca^+ ions, to repair small defects or to maintain mechanical stability.

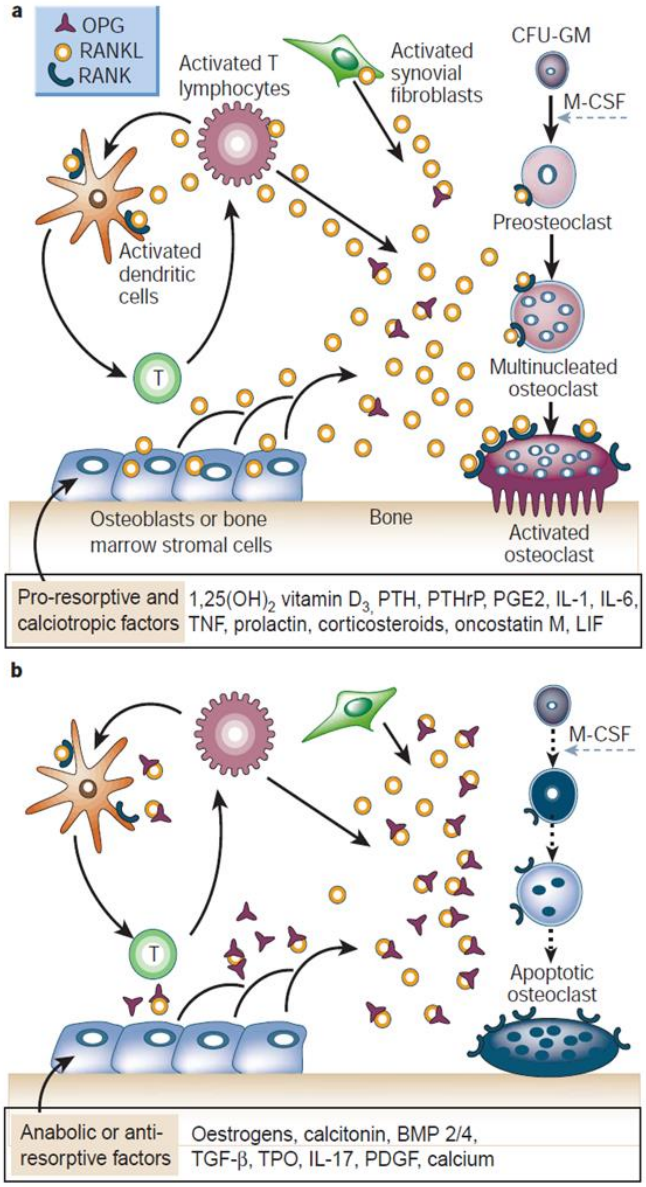

Figure 8: Schematic representation of the hormonal control of bone resorption from Boyle, et al. 2003. It shows the effect of pro-resorptive and calciotropic factors, that increase the RANKL production. In b anabolic or anti-resorptive factors inhibit the osteoclast formation and survival by increased OPG secretion.

This constant resorption and rebuilding cycle of the bone is also called 'bone remodelling'. How do cells know where remodelling is necessary? Several different forms of communication to transmit this information are known: Bidirectional cell-to-cell contact, cytokines, or communication through matrix stored factors (Teti 2013). If the cytokines are secreted by osteoclasts, they are also called clastokines. The most well-known signalling molecules secreted by osteoblasts are M-CSF and RANKL. Additionally

osteoclasts can express the EphrinB2 ligand which stimulates osteoblast differentiation (Teti 2013).

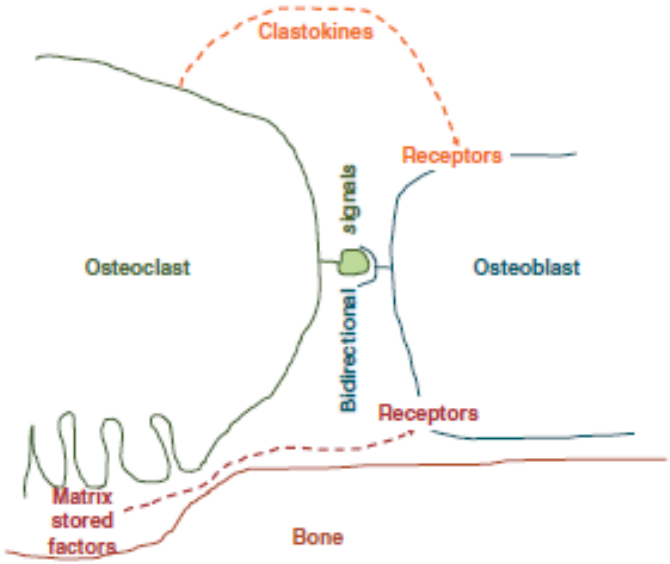

Figure 9: Schematic representation of putative pathways involved in osteoclast-dependent bone formation from Teti 2013.

Abnormal functioning of the cells can lead to various diseases. One of the most common metabolic bone diseases is osteoporosis. Increased osteoclast activity leads to bone loss while osteoblastic bone formation might be reduced. This imbalance leads to a decrease in bone mass and thus increased fracture risk. Therapies for osteoporosis can be separated in two classes: Anabolic drugs, to stimulate the formation of new bone or anti-resorptive drugs to slow down osteoclast activity. In the latter class, bisphosphonates are the most widely used drugs, because they are relatively cheap and applicable for a wide range of osteoporosis patients (Rachner, et al. 2011). But long-term bisphosphonate therapy might also be able to induce skeletal fragility in patients due to the formation of an abnormally dense bone structure (Tolar, et al. 2004, Visekruna, et al. 2008).

One other example for abnormal cell balance would be osteopetrosis, a genetic disease where bone and cartilage are growing excessively. Abnormal functioning of the osteoclasts is the underlying cause of this disease. Depending on the mutation sites the osteopetrosis can be osteoclast-rich or osteoclast-poor. In the osteoclast-rich osteopetrosis the number of osteoclasts can even be higher than normal, but the cells are not able to resorb bone matrix (Teti and Econs 2017). When osteoclasts are still

present, even if they are not actively resorbing, bone formation is higher than in osteoclast-poor patients, where mineralization is decreased, and the organization of osteoblasts is abnormal (Charles and Aliprantis 2014). This led to the hypothesis that osteoclasts play an important role in osteoblast regulation, even if they are not actively resorbing.

Clastokines supported by *in vivo* data			
Factor		***Evidence for effect on bone formation***	***Citation***
CTHCR1	collagen triple repeat containing 1	CTHCR1 is produced by mature OC and stimulated OB differentiation in cell and organ cultures OC specific deletion of *Cthrc1* resulted in decreased BFR and BV/TV	[33, 34]
C3a	complement component 3a	C3 identified as an OB differentiation promoting factor in OC conditioned media C3a promotes OB differentiation *in vitro* A C3aR antagonist augmented bone loss after ovariectomy by reducing BFR	[35]
S1P	sphingosine-1-phosphate	S1P promotes OB differentiation Increased S1P from cathepsin K deficient OCs augmented OB differentiation *in vitro* OC specific $Ctsk^{-/-}$ have increased OB numbers and BFR	[29, 36, 37]
Sema4D	semaphorin 4D	OCs express Sema4D $Sema4d^{-/-}$ OC conditioned media promotes, and Sema4D inhibits, OB differentiation $Sema4d^{-/-}$ mice have increased BFR and BV/TV, which is rescued by BM transplant Sema4D antibody reduces bone loss after ovariectomy	[119]
TRAcP	tartrate resistant acid phosphatase	Secreted TRAcP promotes OB differentiation TRAcP overexpressing transgenic mice have increased BFR $Tracp^{-/-}$ mice phenotype suggests role in endochondral ossification	[120–122]
CT-1	cardiotrophin-1	OC express CT-1 CT-1 promotes OB differentiation Neonatal $Ct\text{-}1^{-/-}$ have decreased OB numbers and BV/TV	[123]
Clastokines supported by *in vitro* data only			
CXCL16	chemokine (C-X-C motif) ligand 16	CXCL16 identified as an OB pro-migratory factor in TGFβ1 treated OC conditioned media	[124]
LIF	leukemia inhibitory factor	OC derived LIF suppresses TGFβ1 induced OB migration	[124]
afamin	afamin	Expressed by OC Promotes OB cell line migration *in vitro*	[125]
BMP6	bone morphogenic protein 6	Induced during OC differentiation Promotes OB differentiation *in vitro*	[37, 126]
Wnt10b	wingless-type MMTV integration site family, member 10b	Induced during OC differentiation Promotes OB differentiation *in vitro*	[37]
SOST	sclerostin	Sclerostin is higher in conditioned media of OCs prepared from aged versus young mice and correlates with inhibition of mineralization Sclerostin neutralizing antibodies relieve mineralization inhibition by OC conditioned media from aged mice	[127]
HGF	hepatocyte growth factor	Expressed by OC Promotes OB proliferation	[128, 129]
PDGF-BB	platelet derived growth factor BB	Produced by non-resorpbing OC Induces MSC/OB precursor migration Inhibits OB differentiation.	[130–132]

Table 1: A summary of putative clastokines that couple bone resorption to osteoblastic bone anabolism from Charles and Aliprantis 2014.

Actively resorbing osteoclasts liberate matrix-derived growth factors like insulin-like

growth factor 1 (IGF1) from the bone matrix. The increased bone formation seen with non-resorbing osteoclasts lead to the hypothesis that the osteoclasts are also releasing growth factors (Charles and Aliprantis 2014). Cytokines produced by osteoclasts are therefore called 'clastokines'. A good overview of suspected clastokines is the table shown in table 1.

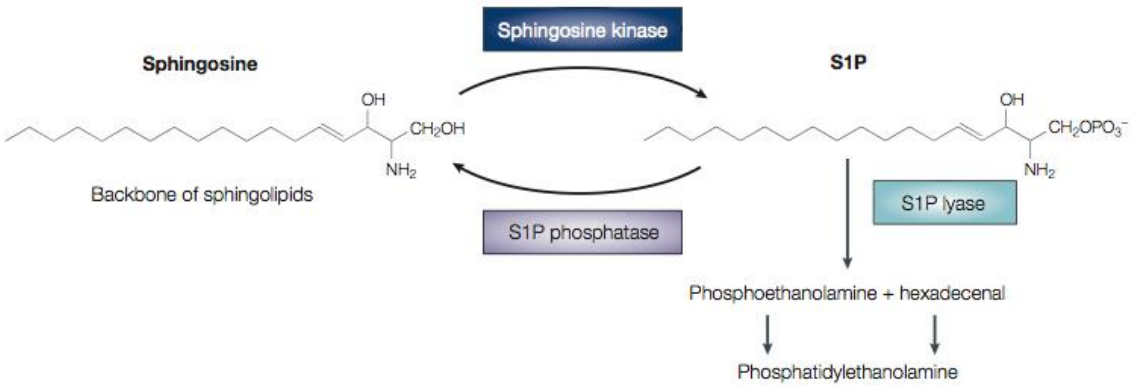

Figure 10: The structures and metabolisation of sphingosine and sphingosine-1-phosphate are shown. Two classes of enzyme are able to degrade sphingosine-1-phosphate (Spiegel and Milstien 2003).

One of those is S1P (Sphingosine-1-phosphate), a ubiquitous signalling molecule that mainly regulates cell growth, suppresses apoptosis and is also involved in cell trafficking. This sphingolipid metabolite is produced by phosphorylation of sphingosine via sphingosine kinases. In mammals the main kinases are sphingosine kinase 1 (SphK1) and sphingosine kinase 2 (SphK2). These also form different isozymes with a high degree of similarity as you can see in figure 11.

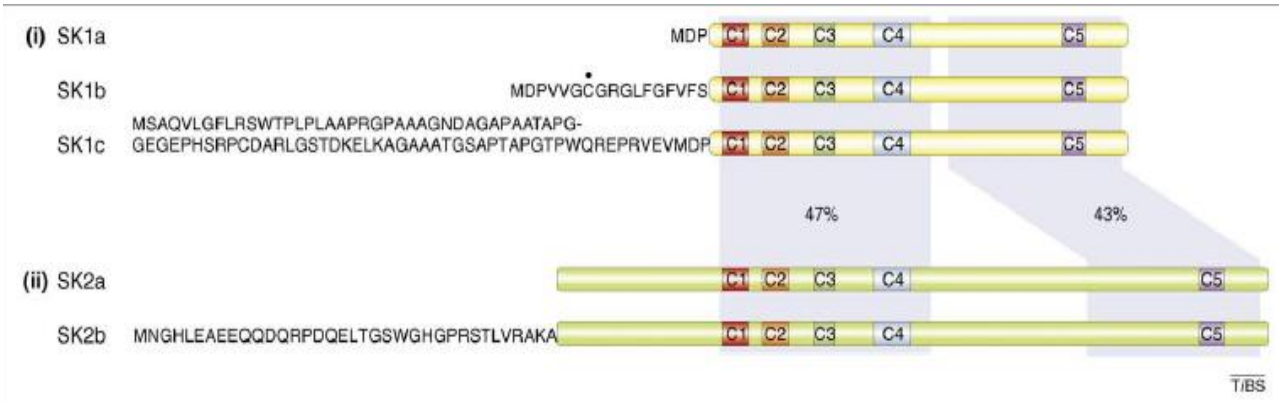

Figure 11: Isoforms of human sphingosine kinase. C1-C5 are highly conserved regions that are found in all known sphingosine kinases (Pitson 2011).

The localization of sphingosine kinase 1 is mainly in the cytoplasm, and in its active state it migrates into the cell membrane. Additionally, the sphingosine kinase 2 is found in the nucleus while it is inactive. Upon activation it migrates to the cytoplasm. It is assumed that the two kinases also have different functions, even though they phosphorylate the same protein. Sphingosine kinase 1 seems to be mainly responsible for cell growth and is more inclined to suppress apoptosis, whereas sphingosine kinase 2 seems to inhibit cell growth and stimulate apoptosis. But experiments in mouse models have shown that the deletion of only one of these kinases produces viable offspring, deletion of both causes the embryos to die in utero between E12.5 and 14.5 due to vascular defects (Mizugishi, et al. 2005). Taken together, it seems as if there is a functional redundancy between these two kinases.

An important activation pathway for both kinases is the ERK1/2 signal, which is stimulated by growth factors or cytokines. This signalling pathway is only active after the phosphorylation of the sphingosine kinase and can phosphorylate sphingosine. This happens at the level of the cell membrane (Pitson 2011). Sphingosine-1-phosphate can then act either directly on the TRAF2 pathway of the cell or be transported outwards via Spns2 (sphingolipid transporter 2) (Keller, et al. 2014). The molecule can act intra- and extracellularly.

Five members of the EDG (endothelial differentiation gene) family have a high affinity for sphingosine-1-phosphate. These G-protein coupled receptors are positioned on the cell membrane; they are also known as Sphingosine-1-phosphate receptors (Pyne and Pyne

2000, Ryu, et al. 2006).

Ryu, et al. 2006 were the first to study the sphingosine-1-phosphate and sphingosine kinases in relation to osteoclasts. They focused on SphK1, as its role in cellular response was better described at the time than that of SphK2. The expression in mouse osteoclast cells during osteoclastogenesis showed an increase over time in protein expression and RT-PCR (real time- polymerase chain reaction). In consecutive experiments they observed that the exogenous addition of S1P to osteoclast cultures inhibited differentiation, whereas the addition of S1P to a co-culture of osteoblasts and osteoclasts was inducing osteoclastogenesis.

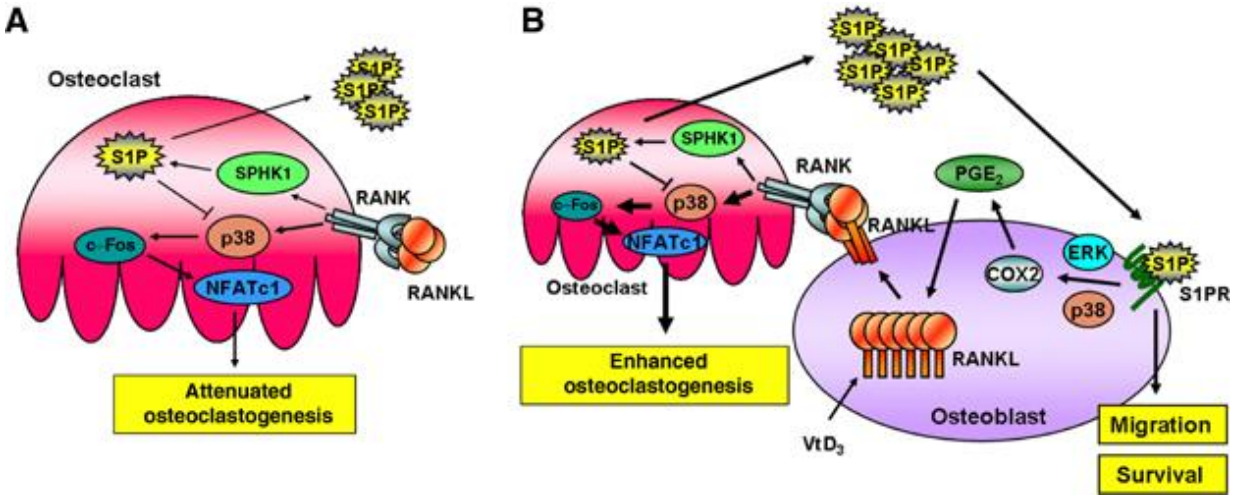

Figure 12: Schematic diagrams for osteoclastogenesis modulation proposed by Ryu, et al. 2006. Figure 12A shows the inhibitory effect of excess sphingosine-1-phosphate on single osteoclast cultures through a negative feedback loop. Figure 12B shows the positive influence of sphingosine-1-phosphate on osteoblast survival and in turn the increased production of RANKL, which enhances osteoclastogenesis.

In the figure 12 B the model proposed by the group around Ryu shows that enhanced osteoclastogenesis is induced by an increase in RANKL secretion by osteoblasts. If no osteoblasts are present the S1P production is increased but has a negative effect on osteoclastogenesis. Many other groups also looked at the influence of S1P and SphK1 on osteoclasts (Ishii, et al. 2009, Ishii, et al. 2010, Keller, et al. 2014, Lotinun, et al. 2013, Shiwaku, et al. 2015). The group around Keller, et al. 2014 tested the influence of calcitonin receptors on S1P and its expression. They found that mice lacking the calcitonin receptor showed an increase in S1P levels and less bone formation. Pederson,

et al. 2008 investigated the clastokines in RAW 264.7 cells as well as primary mouse osteoclasts. After performing an expression study using an Affymetrix microarray they chose Wnt10b, BMP6 and S1P as the most promising factors.

Using western blot, they saw a significant increase of SphK1 during osteoclastogenesis in both cell types. Another group generated a cathepsin K conditional knockout mouse. They saw an increase in SphK1 expression and subsequently an increase in bone formation in these mice (Lotinun, et al. 2013). To see if the growth surface of osteoclasts can influence the coupling factor secretion, the group of Shiwaku, et al. 2015 cultured cells on biphasic calcium phosphates with different compositions and compared it to dentin. They saw an increase in expression in some coupling factors, one of them being SphK1, and the supernatant of these cultures was also able to increase mineralization in osteoblast cultures. Ishii and colleagues performed several experiments using RAW 264.7 cells as osteoclast precursor cells to observe the influence of S1P on their mobility. Positive chemotaxis was observed along a S1P gradient, but very high S1P concentrations, as are present in the blood, lead to negative chemotaxis (Ishii, et al. 2009, Ishii, et al. 2010).

The clastokines are a relatively big research topic, and there are also publications that could not find a systemic influence of a sphingosine-1-phosphate analogue (FTY720, Fingolimod) on fracture healing in mice (Heilmann, et al. 2013). The reason might be that FTY720 is metabolised primarily by SphK2 whereas SphK1 is thought to be the more important kinase in osteoclast signalling (Billich, et al. 2003, Ryu, et al. 2006).

It was the aim of this study to examine the expression of SphK1 in primary mouse cells and the RAW 264.7 cell line to see if the increased expression during osteoclastogenesis could be found.

3. Methods and Material

3.1 Methods

3.1.1 Experimental design

To be able to study the potential differences between undifferentiated cells, osteoclast precursor cells and mature osteoclasts we had to choose three time points where the desired cells were present. These time points were selected based on the time the different cells needed to mature. RAW 264.7 cells produced mature osteoclasts on day 4, so the precursor cells were present on day 2. The control group also represented the undifferentiated macrophages. Mouse bone marrow-derived macrophage (BMM) cultures and co-cultures of osteoblast and osteoclast precursors both produced mature osteoclasts on day 5. Since we were able to harvest enough cells on day 1 in the co-culture, day 1 represented the undifferentiated stage for our experiments. In the BMM culture the control group supplemented with rhM-CSF (recombinant human macrophage colony stimulating factor) showed undifferentiated mononuclear macrophages. In both culture models osteoclast precursor cells were harvested on day 3 and mature osteoclasts on day 5.

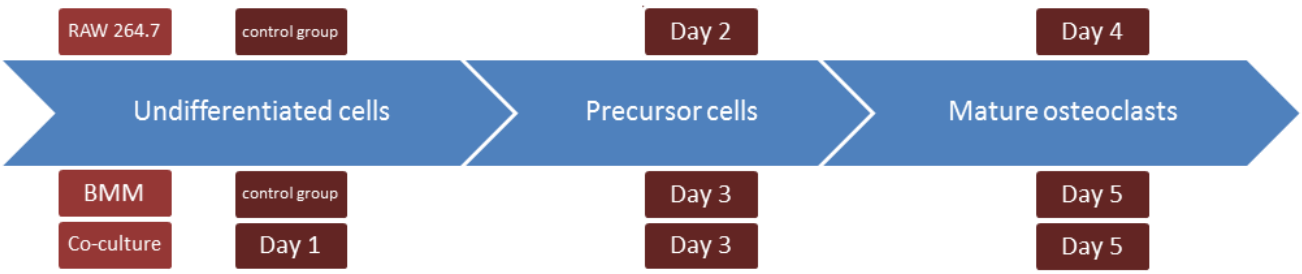

Figure 13: Overview of the experimental design used for this thesis. BMM are bone marrow-derived macrophages from BALB/c mice.

The animals sacrificed for these experiments were 2-month-old BALB/c mice. All steps in the cell culture were performed under sterile conditions in a laminar flow hood and the cultures were maintained at 37 °C in an atmosphere with 5 % CO_2.

The validation of the SphK1 antibody was done with RAW 264.7 cells as they are listed as positive control in the data sheet. Since it's a cell line it had to be validated for our specific strain. We also had to find the optimal antibody concentration for our working protocol.

To be able to show the different amounts of osteoclasts at each time point and enumerate the osteoclasts per cm^2 additional cultures for TRAP (tartrate-resistant acid phosphatase) staining were done in parallel to the cultures for the cell lysis.

3.1.2 rmRANKL-mediated osteoclast formation in RAW 264.7 cells

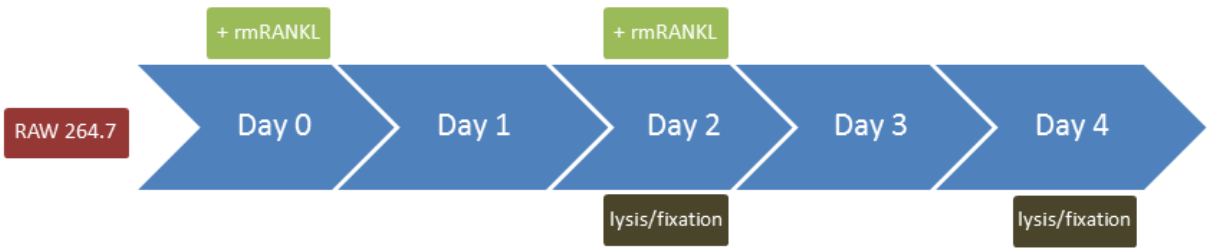

Figure 14: Overview of the experimental design for the RAW 264.7 cell culture.

RAW 264.7 cells are a mouse macrophage cell line that differentiates into osteoclasts in the presence of RANKL (receptor activator of nuclear factor 'kappa-light-chain-enhancer' of activated B-cells ligand). The seeding density was 80 000 cells/cm^2. The cells were cultured in culture medium for 48 hours. Then, at the first medium change rmRANKL (recombinant mouse RANKL) was added at a concentration of 7.5 ng/ml. The control group of RAW 264.7 cells was cultured under the same conditions but without addition of rmRANKL.

As this cell line grows faster than mouse bone marrow-derived macrophages, the fusion reached its peak after 4 days. On day 2 cells were lysed or fixed to represent the osteoclast precursor state, on day 4 the same was done to the mature osteoclasts. The cell lysate was used for protein separation via gel electrophoresis and fixed cells were TRAP stained for enumeration.

3.1.3 rmRANKL mediated osteoclast formation from mouse bone marrow-derived osteoclast precursors

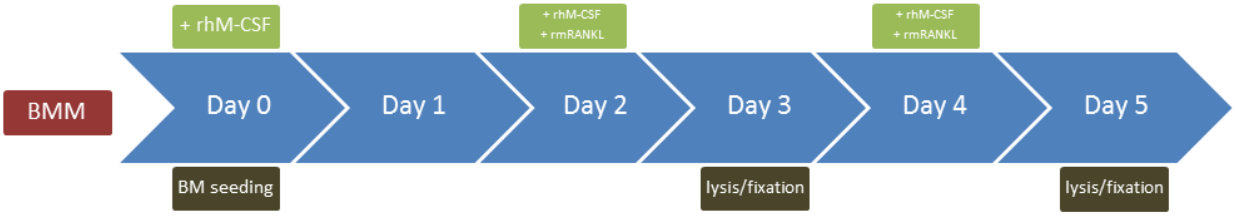

Figure 15: Overview of the experimental design for the mouse osteoclast culture from bone marrow-derived macrophages (BMM).

Mouse bone marrow-derived osteoclast precursor cells were isolated from the femora and tibiae of 2-month-old BALB/c mice. The bone marrow was flushed from the long bones with a sterile syringe using a 27G needle. The collected cells were then centrifuged for 5 minutes at 1000 g. The red blood cells were lysed to obtain a cleaner culture. The seeding density for this culture was 160 000 cells / cm². The cells were seeded in culture medium supplemented with 30 ng/ml rhM-CSF for 48 hours. Then 30 ng/ml rmRANKL was also added to the culture medium in the sample group, the control group only received rhM-CSF.

Cells harvested from BALB/c mice needed 5 days to form mature osteoclasts. On day 3 cells were lysed or fixed to examine the osteoclast precursors. On day 5 the mature, multinucleated cells were also either fixed or lysed. The cell lysate was separated using gel electrophoresis and the fixed cultures were later TRAP stained to be counted.

3.1.4 Mouse osteoclast formation in co-culture with osteoblasts

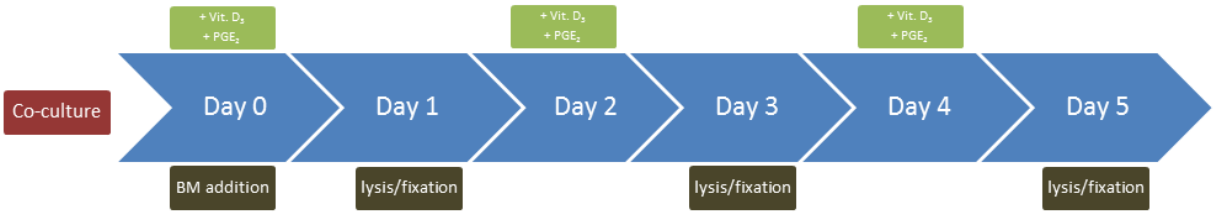

Figure 16: Overview of the experimental design of the mouse osteoblast-osteoclast co-culture. Mouse osteoblasts were cultured with mouse bone marrow-derived cells.

For the co-culture of osteoblasts and osteoclasts we used primary mouse cells. The osteoblasts were isolated from the calvariae of neonatal 1-2 day old mice. Briefly, the cells were fractioned with a dispase/collagenase solution and fractions II, III and IV were collected. After one round of splitting the cells were kept in frozen nitrogen. For the co-culture the osteoblasts were seeded at a density of 74 000 cells / cm². After a 24-hour attachment period mouse osteoclast precursor cells from bone marrow were added. The isolation of these cells was carried out as described above, but without the red blood cell lysis. The collective bone marrow from two mice was enough for one 6-well culture plate. The culture medium was made with FCS (fetal calf serum). It was supplemented with 10 µM 1,25-dihydroxyvitamin D3 and 1 mM prostaglandin E2.

The co-culture consisted of primary mouse cells and was therefore cultured until day 5. Due to the larger number of cells in each well we were able to lyse or fix cells already on day 1 already. On day 3 we lysed the cells to obtain osteoclast precursors or fixed them. On day 5 the same procedure was performed to obtain mature osteoclasts. The cell lysates were separated using gel electrophoresis and the fixed cells were TRAP stained for further quantification.

3.1.5 TRAP staining and counting

To evaluate the osteoclast differentiation, cultured cells were stained for TRAP, an osteoclastic enzyme widely used to identify osteoclasts. Therefore, cells were washed

with PBS (phosphate buffered saline) and fixed with a 10 % buffered formalin solution for 10 min. at room temperature. After fixation, cells were washed three times with PBS with added $Ca^{2+}$and $Mg^{2+}$and either stained immediately or stored in PBS (with Ca^{2+}/Mg^{2+}) at 4 °C until the staining.

For the TRAP staining, the fixed cells were incubated with TRAP buffer at 37 °C for 30 min. and then treated with an ethanol/acetone solution (1:1) for 30 seconds to permeabilize the cell membrane. After complete drying of the culture plate the cells were incubated with TRAP staining solution for 10 min. at 37 °C. To stop the staining reaction the cells were washed three times with distilled water. The plates were then stored in distilled water containing 1 % sodium azide at 4 °C until quantification. To quantitate mature osteoclasts, TRAP positive stained cells with three or more nuclei were enumerated using an inverted light microscope at a 10X magnification.

3.1.6 Cell lysis

For the immunoblotting the cells had to be lysed, as the sphingosine kinase is found mostly in the cell membrane and cytoplasm (Pitson 2011). Cell lysis was done with RIPA (radioimmunoprecipitation assay) buffer, containing NaF (50 µM), aprotinin (40 µg /ml), leupeptin (1 µg / ml), pepstatin (1 µg / ml), sodium orthovanadate (2 mM) and PMSF (phenylmethylsulphonyl fluoride, 1 mM). Cells were washed three times with cold PBS, which was then completely removed. RIPA buffer was added to the well. The cells were detached from the plastic dish using a cell scraper. The obtained cell suspension was then incubated for one hour on ice while shaking on a vortex mixer every ten minutes. The solution was centrifuged for 15 minutes at 13 500 rpm and the collected supernatant frozen at -20°C.

3.1.7 Gel electrophoresis and western blot

To ensure equal loading for the western blot the protein content of each sample had to be measured. We used the BioRad® DC™ Protein assay and mixed 5 µl of our samples with the solutions according to the manufacturer's instructions. The absorption was

measured at 690 nm. For each run a standard consisting of RIPA buffer with known concentrations of BSA was added to create a standard curve for each experiment.

Before the gel electrophoresis we prepared our samples by mixing them with sample buffer containing SDS (sodium dodecyl sulphate) and heating them to 95 °C for 5 minutes. Proteins were loaded at different amounts depending on the culture system, varying in between 30 µg and 75 µg per lane. They were separated via gel electrophoresis on a 10% polyacrylamide gel. Protein transfer was done in a wet tank blotting onto a nitrocellulose membrane. Unspecific binding sites were blocked with a 5% milk blocking solution for one hour at room temperature. Incubation with primary antibody against SphK1 at a concentration of 1:100 was done overnight at 4°C. The secondary antibody was an anti-mouse IgG (immunoglobulin G) HRP (horse radish peroxidase)-conjugate at a dilution of 1:2000. Incubation time was one hour at room temperature. Detection differed between the primary cell lysates and the RAW 264.7 cell groups. RAW 264.7 cell lysate blots were detected with X-ray film. For a loading control the housekeeping protein beta-actin was used. As the molecular weight of this protein is very similar to the molecular weight of SphK1, the membrane had to be stripped. We used a stripping buffer containing β-mercaptoethanol, SDS and Tris (Tris(hydroxymethyl) aminomethane) HCl and stripped the membrane for 30 minutes at 50 °C in a shaking incubator. After a longer washing step and another milk blocking the blot was incubated with primary antibody against beta actin at a concentration of 1:2000 overnight at 4 °C. Incubation with the secondary antibody as well as the detection were done as described above.

The other blots obtained from the lysates of the primary mouse osteoclast cultures and the co-cultures were detected with the ChemiDoc® system from Bio-Rad. A total protein staining was done with Ponceau S solution to account for differences in the loading of the lanes and was scanned using the ChemiDoc® system from Bio-Rad.

The X-ray films were scanned so that all blots could be quantified with the Image Lab software from Bio-Rad. As references we either used the undifferentiated cell lysate or the lysate from day 1 in the case of the co-culture. To be able to compare the values from different western blots we had to normalize the relative intensity values obtained.

We set the references, either day 1 in the co-culture or the undifferentiated cells in the RAW 264.7 cell culture and the BMM cell culture, to 100 %.

3.1.8 Statistical analysis

Cell numbers generated by counting TRAP positive multinuclear cells were analyzed with Prism 5.0c software. Band intensities from western blot detection were generated with Image Lab 6.0 software from Bio-Rad. The obtained numbers were also analyzed with the Prism 5.0c software. P-values were calculated using Tukey's post-hoc test. The results were not considered significant if $p>0.05$.

3.2 Material

3.2.1 Tools

Table 2: Tools used in the experiments:

Tool	**Company**	**Country**
Autoclave SX-300E	Tomy Digital Biology	JPN
CASY TT Cell counter & analyser	OLS OMNI Life Science	GER
ChemiDoc™ Imaging System	Bio-Rad	GER
Costar 3010 cell scraper	Corning Incorporated	USA
Digital camera ProGres Speed XT Core5	Jenoptik	GER
Drying cabinet	Binder WTB	GER
Film drying closet	Kindermann	GER
Gel pouring stand	Bio-Rad	GER
Heating block	Eppendorf	AUT
Ice flaker AF103	Scotsman Ice Systems	USA
Incubator Hera Cell 240	Thermo	USA
Laminar flow hood	Ehret	GER
Light optical microscope H550S	Nikon TMS	JPN
Magnetic stirrer	Heito	FRA
Magnetic stirrer RCT	Janke & Kunkel	GER
MegaStar 600R centrifuge	VWR International	USA
Microbalance MC210 P	Sartorius	GER
Micropipettes	VWR International	AUT
Microtiterplate reader Infinite 200	Tecan	CH
Mini-Protean Tetra vertical electrophoresis cell	Bio-Rad	GER
Mini-Protean Trans-Blot Cell	Bio-Rad	GER
Pipetboy pipetting aid	Integra Bioscience	GER

Pipettes	Gilson	FRA
Power Pac 200	Bio-Rad	GER
Quick centrifuge	Labnet	USA
Shaking incubator 3032	GFL	GER
Shaking plate	Bühler	GER
Vortex-Genie 2	Bender & Hobein	GER
Ultrasonic bath Transsonic 570	Elma	GER
Vortex-genie 2	Bender & Hobein	GER
Water bath 1083	GFL	GER
X-ray cassette	Amersham Biosciences	USA

3.2.2 Materials

Table 3: Materials used in the experiments:

Material	**Company**	**Country**
6-Well plate tissue culture	Greiner Bio-One	AUT
48-Well plate tissue culture	Greiner Bio-One	AUT
10 well comb	Bio-Rad	GER
Blotting paper	Schleicher & Schuell	GER
CASY Cup	Roche Diagnostics	GER
Centrifugal tubes 15 ml	Greiner Bio-One	AUT
Centrifugal tubes 50 ml	Greiner Bio-One	AUT
Eppendorf tubes	Eppendorf	AUT
Filter paper	Schleicher & Schuell	GER
Glass pipette	Brand	GER
Glass plate		
Nitrocellulose membrane	Schleicher & Schuell	GER
Para film	Sigma-Aldrich	AUT
Petri dishes round	Greiner Bio-One	AUT
Petri dishes squared	Greiner Bio-One	AUT
Pipetting tips	VWR International	AUT

Scalpel	Bard-Parker	USA
Sheet protector	Bene	AUT
Single use needles 27G x ¾ in.	BD	IRL
Single use syringe 1 ml	Henke Sass-Wolf	GER
Transparent 96-well microtiterplate	Greiner Bio-One	AUT
Water scale AZB40	SOLA	AUT
X-ray film	Kodak	USA

3.2.3 Reagents

Table 4: Reagents used in the experiments:

Reagents	**Lot Nr.**	**Company**	**Country**
1,25-dihydroxyvitamin D_3	#R0 21-5535	Roche	AUT
Acetone	#121164098	Roth	GER
Acrylamide	#79061	Sigma-Aldrich	AUT
Alpha-MEM	#22571-020	Gibco LifeTechnologies	AUT
Ammonium persulfate	#7727540	Sigma-Aldrich	AUT
Anti-mouse IgG HRP-conjugate	#M4280	Sigma-Aldrich	AUT
Aprotinin	#87H7011	Sigma-Aldrich	AUT
Bovine serum albumin	#EG2923225	Roth	GER
Bromophenol blue	#115393	Sigma-Aldrich	AUT
CaCl2	#97H0981	Sigma-Aldrich	AUT
CASYton	#11689200	Roche Diagnostics	GER
Clarity™ Western ECL Substrate	#170-5060	Bio-Rad	USA
Collagenase 0.1%	#075M4045V	Sigma-Aldrich	AUT

Developer solution	#G354	AGFA	BEL
Dimethyl sulfoxide	#BCBJ4366V	Sigma-Aldrich	AUT
Dispase neutral protease grade II	#14927900	Roche	JPN
EDTA	#50K01315	Sigma-Aldrich	AUT
EtOH 70%		AustrAlco	AUT
EtOH 99.99%		AustrAlco	AUT
Ethylenediaminetetraacetic acid	#60004	Sigma-Aldrich	AUT
Fast Red Violet LB Salt	#MKBH6351V	Sigma-Aldrich	USA
FCS BM	#084M3250	Sigma-Aldrich	USA
FCS HI	#084M3250	Sigma-Aldrich	USA
Fixing solution	#G334	AGFA	BEL
Glycerine	#7098808	Sigma-Aldrich	AUT
Glycine	#56406	Sigma-Aldrich	AUT
H_2O_2	#822287	Merck	AUT
HCl	#2202004061000	Chem-Labs	BEL
KCl	#K33076636428	Merck	GER
KH_2PO_4	#851A386673	Merck	GER
Leupeptin	#26H0892	Sigma-Aldrich	GER
Methanol	#1.06009	Merck	GER
$Na_2HPO_4*2H_2O$	#K33351980429	Merck	GER
NaCl	#236241234	Sigma-Aldrich	GER
NaF	#S-6776	Sigma-Aldrich	AUT
Na-desoxycholat	#97H0027	Sigma-Aldrich	AUT
$NaHCO_3$	#035K0074	Sigma-Aldrich	GER
N,N-dimethylformamid	#5HBC5480V	Sigma-Aldrich	USA
NaOH	#2129930051000	Chem-Labs	BEL
Naphthol AS phosphate	#061M5303V	Sigma-Aldrich	USA
Na-o-Vanadat			
PageRuler Prestained	#26616	Thermo-	USA

Protein Ladder		Scientific	
Penicillin /Streptomycin 10,000 U/ml /10,000 µg/ml	#15240-062	Biochrom	GER
Pepstatin A	#P4265	Sigma-Aldrich	AUT
Phenylmethylsulfonyl fluoride	#P-7626	Sigma-Aldrich	GER
Ponceau S powder	#MKCF4831	Sigma-Aldrich	AUT
Prostaglandin E_2	#0469181-75	Cayman Chemical Company	USA
RBC (red blood cell) lysis Buffer	#1074900	Roche	GER
Protein Assay, Reagent A	#500-0013	Bio-Rad	GER
Protein Assay, Reagent B	#500-0114	Bio-Rad	GER
Protein Assay, Reagent S	#500-0115	Bio-Rad	GER
Recombinant human M-CSF	#ME093121	R&D System	USA
Recombinant murine RANKL	#CWA181512	R&D System	USA
Skim milk powder		Maresi	AUT
Sodium acetate	#93H0417	Sigma-Aldrich	AUT
Sodium azide	#94H2685	Sigma-Aldrich	USA
Sodium citrate	#STBF1932V	Sigma-Aldrich	AUT
Sodium dodecyl sulphate ultra-pure	#151-21-3	Roth	GER
Sodium tartrate	#82H06941	Sigma-Aldrich	AUT
Sphingosine Kinase 1 (G-11) antibody sc-365401	#H1017	Santa-Cruz	USA
Tetramethylethylenediamine	#161-0800	Bio-Rad	AUT
Trichlor acetic acid	#200-927-2	Roth	AUT
Tris (Tris(hydroxymethyl) aminomethane) base	#77861	Sigma-Aldrich	AUT
Triton X-100	#106H6019	Sigma-Aldrich	AUT

Tween 20	#SZBE2460V	Sigma-Aldrich	AUT

3.2.4 Preparation of solutions

- **0.1% Bovine serum albumin in PBS with Ca^{2+}/Mg^{2+}**: 0.01 g BSA were dissolved in 10 ml PBS with Ca^{2+}/Mg^{2+} and sterilized by filter sterilization.
- **1X Lysis buffer:** 0.5 ml 10X RBC Lysis buffer solution was diluted with 4.5 ml ultrapure water to 1X.
- **1X sample buffer:** the 4X sample buffer was diluted to a ratio of 1:3 with dH_2O and portioned into Eppendorf tubes and stored at -20°C.
- **1X TBS buffer:** 100 ml 10X TBS buffer were diluted with dH_2O to 1 000 ml. The buffer was stored at 4 °C.
- **4X sample buffer:** 1.52 g tris base, 9.45 g glycine and 0.116 g EDTA were dissolved in 40 ml dH_2O and adjusted to pH 6.9 with HCl. Then 6 g SDS and 0.2 g bromphenolblue were added and diluted with dH_2O to a volume of 50 ml. At the end 50 µl beta-Mercaptoethanol was added. The buffer was portioned into Eppendorf tubes and stored at -20 °C.
- **10% APS:** 0.1 g ammonium persulfate was dissolved in 1 ml dH_2O. The solution was stored at -20 °C.
- **10 % SDS solution:** 10 g SDS ultra pure was dissolved in dH_2O and then diluted to a volume of 100 ml. The mixture was stored at room temperature.
- **10X running buffer, pH 8.9:** 60.5 g tris base was dissolved in dH_2O and 285.5 g glycine was added as well as 40.0 g SDS. The pH was adjusted to 8,9. At the end dH_2O was added to reach a volume of 2 l. The solution was diluted with dH_2O before use to a ratio of 1:10.
- **10X TBS buffer:** 12.1 g tris base and 40 g NaCl were dissolved in 500 ml dH_2O. The pH was adjusted to 7.4 with 32 % HCl. The mixture was stored at 4 °C.
- **500X NaN_3 solution:** 0.1 g sodium acid was dissolved in 1 ml dH_2O. The solution was stored at 4 °C.
- **Blocking buffer:** 1.25 g skim milk powder was dissolved in 25 ml TBST 0.1 % while mixing at 80 °C for about 5 min. For immediate use or stored at 4 °C.

- **Culture medium:** alpha-MEM + 10% FCS: alpha-MEM was mixed with 10% FCS HI (FCS BM in the co-culture) and 1% penicillin-/streptomycin solution and stored in sterile glass bottles at 4 °C. Before use it was warmed to 37 °C in the water bath.
- **Detection solution:** the solution was mixed with tap water 1:3 and stored away from light.
- **Fixing solution:** the solution was mixed with water 1:3 and stored away from light.
- **Loading control antibody solution:** the antibody was solved in blocking buffer
- **Lower Tris, pH 8.8:** 18.7 g tris base was dissolved in 70 ml dH_2O and adjusted to pH 8.8 with 32% HCl. Then 4 ml 10% SDS solution was added and diluted with dH_2O to a volume of 100 ml. The mixture was stored at 4 °C.
- **M-CSF stock solution (R&D system):** the lyophilized M-CSF was centrifuged and solved in 0.1% BSA in PBS with Ca^{2+}/Mg^{2+}. Then it was diluted to a concentration of 10 µg/ml. The solution was dispensed into aliquots and frozen at -80 °C.
- **PBS with Ca^{2+}/Mg^{2+}:** 2 g KCl, 2 g KH_2PO_4, 80 g NaCl, 14.34 g Na_2HPO_4 •2 H_2O and 1 g $MgCl_2$ •6 H_2O were solved in 1000 ml dH_2O. The pH was adjusted to 2-3 with 5 M HCl. Then 1 g $CaCl_2$ was added. This solution was diluted with dH_2O to a final volume of 10 l and then the pH was adjusted to 7.2 with 5 N NaOH.
- **Phosphate-buffered saline (PBS):** 2 g KCl, 2 g KH2PO4, 80 g NaCl and 27.07 g Na_2HPO_4 •2H_2O dissolved in 1000 ml dH_2O then add dH_2O to 10 l. Filter sterilization to sterilize the solution.
- **Ponceau staining solution 0,2 %:** 0.2 g Ponceau S powder and 10 ml acetic acid (99%) were mixed and filled up to 200 ml with dH_2O. From this 20X stock 0.75 ml were again diluted with water to create a 1X solution for use.
- **Primary antibody solution:** 0.2 g BSA was dissolved in 5 ml TBST 0.1 % on the magnetic mixer. 4 ml of this solution were mixed with 8 µl NaN_3 solution (to stabilize) and 4 µl Sphk1 antibody (Santa Cruz Biotechnology, Inc; sc-365401) to reach a concentration of 1:100.
- **RANKL stock solution (R&D system):** the lyophilized RANKL was centrifuged and solved in 0.1% BSA in PBS with Ca^{2+}/Mg^{2+}, then diluted to a concentration of 10 µg/ml. The solution was dispensed into aliquots and stored at -80 °C.
- **Reagent A':** 40 µl reagent S was mixed with 2000 µl reagent A.

- **RIPA buffer:** 0.462 g NaCl, 0.061 g Tris base and 0.073 g EDTA were solved in 50 ml dH_2O. The pH was adjusted to 7.2 and then 0.5 g Triton X-100, 0.5 g Na-desoxycholate and 0.05 g SDS were added. The solution was stored at + 4 °C.
- **Secondary antibody solution:** mixed 2 ml blocking buffer and 1 µl Anti-Mouse IgG HRP-Conjugate for a 1:2000 antibody solution.
- **Standard curve:** BSA was solved in RIPA buffer in 8 different concentrations: 0 µl/ml, 0.25 µl/ml, 1 µl/ml, 1.5 µl/ml, 2 µl/ml and 2.5 µl/ml, and stored at -20 °C.
- **Starvation medium:** alpha-MEM + 0,5% FCS: alpha-MEM was mixed with 0,5 % FCS HI (or FCS BM in the co-culture) and 1% penicillin-/streptomycin solution. The starvation medium was stored in a sterile glass bottle at 4 °C and warmed to 37 °C before use.
- **Stripping buffer:** 4,665 g Tris HCl was solved in 400 ml dH_2O and the pH adjusted to 6,8. 10 g of SDS and 100 ml dH_2O were added. Shortly before use 700 µl beta mercaptoethanol for 100 ml buffer solution were added.
- **TBST 0.1%:** 1 ml Tween 20 was dissolved in 1 000 ml 1X TBS. The mixture was stored at 4 °C.
- **Transfer buffer:** 18 g glycine and 3.7 g tris base were dissolved in 2l dH_2O. The pH was measured and if necessary adjusted to 8.3-8.4. Then 500 ml of methanol were added. The solution was stored at 4°C.
- **TRAP buffer:** for 100 ml TRAP-buffer 0.5444 g sodium acetate were dissolved in dH_2O. The pH was adjusted to 5.0 with 1 M HCl. Then 0.2302 g sodium tartrate was added.
- **TRAP staining solution:** for each staining a fresh solution was prepared. 5 mg naphthol AS phosphate were mixed with 500 µl N,N-dimethylformamide and vortexed until the solution became clear. From this mixture 80 µl were added to 8 ml TRAP buffer. Then 4.8 mg Fast Red Violet Salt was also added to the TRAP buffer and mixed for 5 min in an ultrasonic bath. The solution was stored away from light until use.
- **Upper Tris, pH 6.8:** 6.06 tris base was dissolved in 70 ml dH_2O and adjusted to pH 6.8 with 32 % HCl. Then 4 ml 10% SDS solution were added and diluted with dH_2O to a volume of 100 ml. The mixture was stored at 4°C.

- **Washing medium:** alpha-MEM + 2% FCS: alpha-MEM was mixed with 2% FCS HI and 1% penicillin-/streptomycin solution. The washing medium was stored in a sterile glass bottle at 4 °C.

4. Results

4.1 Experimental design

The original hypothesis was that the amount of SphK1 in the osteoclast increases during osteoclastogenesis (Pederson, et al. 2008, Ryu, et al. 2006). There are 3 main stages of differentiation the osteoclasts go through. First the cells are undifferentiated macrophages, then osteoclast precursor cells are formed and finally mature osteoclasts. The first model we used was a RAW 264.7 cell culture. As these cells are derived from a cell line they differ from primary mouse cells in some respects. For example, RAW 264.7 cells do not need additional M-CSF (macrophage colony stimulating factor) to differentiate into macrophages. Another culture system we looked at was a co-culture of osteoblasts and osteoclasts with supplemented 1,25-dihydroxyvitamin D_3 and prostaglandin E_2. In this model the cells are cultured together and might behave differently compared to a single cell culture (Ryu, et al. 2006). To study the cytokine secretion of primary mouse osteoclasts we first needed to establish a culture model for mouse bone marrow derived osteoclasts. The goal was to obtain a significant number of mature, multinucleated osteoclasts after 5 days. We obtained the best results with a supplementation of 30 ng/ml of each rhM-CSF and rmRANKL and a seeding density of 160 000 cells/cm^2.

We wanted to optimize the protein yield from cell lysis, so we tested different lengths of incubation time with the lysis buffer. The three time points we chose were 15 min, 30 min and 60 min. Figure 17 shows that after 60 min of incubation time the yield of our protein of interest increased by about 26 %. Based on this finding we used a 60 min incubation time for all subsequent experiments.

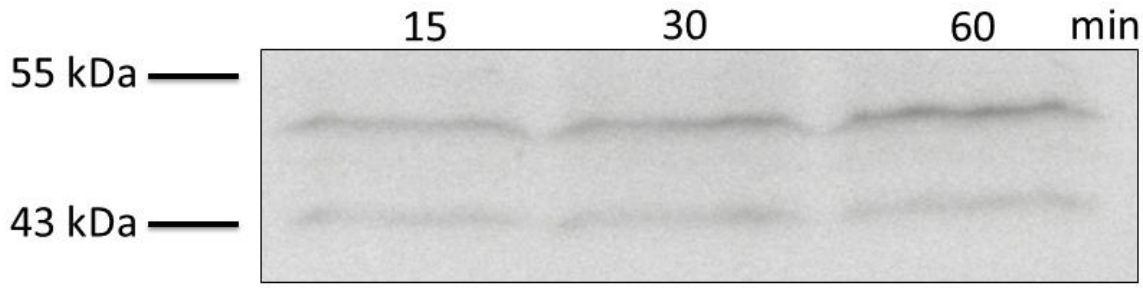

Figure 17: Comparison of different incubation lengths with lysis buffer. RAW 264.7 cell lysates were incubated with RIPA buffer for 15, 30 or 60 min and then separated on a 10 % acrylamide gel. Western blot detection was done using a SphK1 antibody.

4.2 RAW 264.7 cell culture

To show that mature, multinucleated osteoclasts are present on day 4 we cultured a part of the cell batch for a TRAP staining in parallel to the cell lysis on days 2 and 4. Figure 2 shows that there is some difference between cells that were serum starved for 24 h and cells that were continuously cultured with 10 % serum. The cells that had not been starved present a slightly better morphology (Figure 19), but counting TRAP positive multinuclear cells showed that the difference in the number of multinucleated cells was not statistically significant. The osteoclast density in the starvation group was slightly lower (663 OC/cm²) than in the positive control group (820 OC/cm²). On the other hand, there are significant differences in the cell morphology as well as the number of TRAP positive multinuclear cells from day 2 to day 4 (Figure 20). Using the osteoclast numbers from the counting TRAP positive cells we were also able to calculate the average number of osteoclasts / cm^2 (Table 5).

Table 5: Osteoclast quantification in a RAW 264.7 cell culture. The +RANKL group was supplemented with 7.5 ng/ml rmRANKL, the S+RANKL group was supplemented with 7.5 ng/ml rmRANKL and starved for 24 hours. TRAP+ multinucleated cells with 3 or more nuclei were counted:

Osteoclasts/cm²	**undifferentiated RAW 264.7 cells**	**+RANKL group**	**S+RANKL group**
day 2	0	19	16
day 4	0	820	663

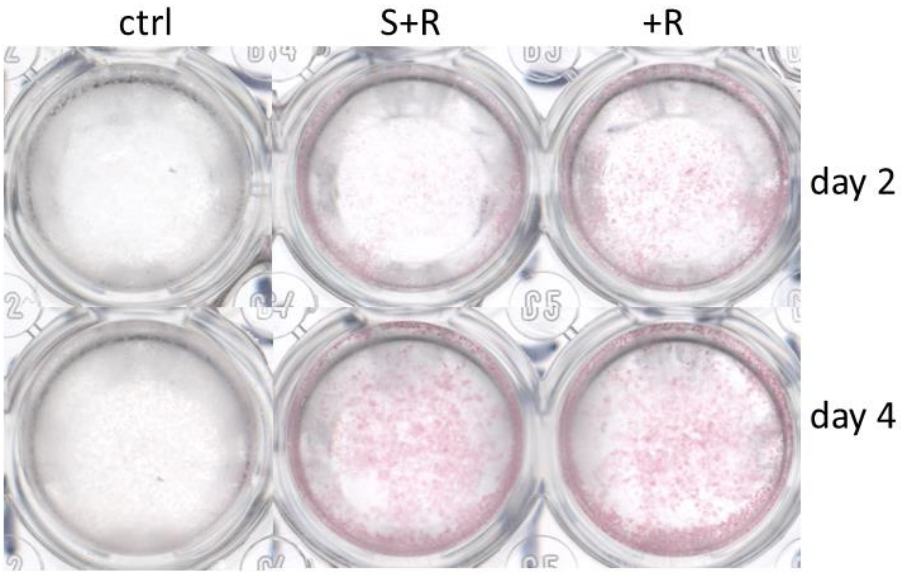

Figure 18: Osteoclast differentiation of RAW 264.7 cells under influence of serum starvation. TRAP staining was done on days 2 and 4. The control group (ctrl) was cultivated in standard culture medium. The S+R group was supplemented with 7.5 ng/ml rmRANKL and starved for 24 hours before fixation. The +R group was cultivated with 7.5 ng/ml rmRANKL, no starvation before fixation.

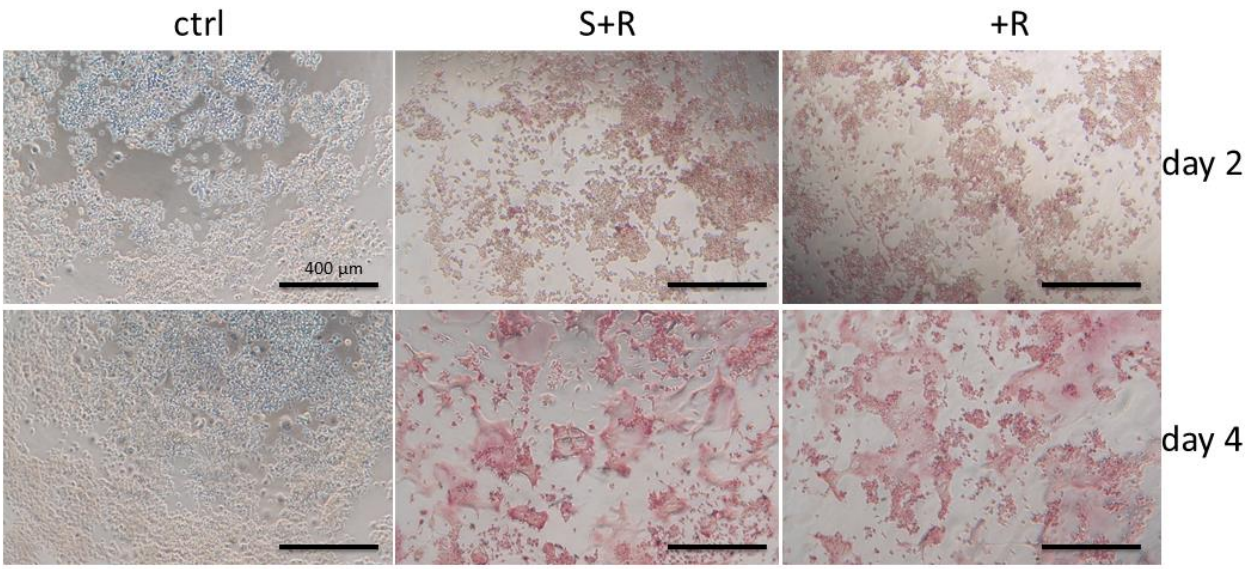

Figure 19: Osteoclast differentiation of RAW 264.7 cells under influence of serum starvation in a 10x magnification. The ctrl group was cultivated using standard culture medium and fixed on day 2 and 4. The S+R group was supplemented with 7.5 ng/ml rmRANKL and starved for 24 hours before fixation. The +R group was cultured with 7.5 ng/ml RANKL, but not subjected to starvation before fixation.

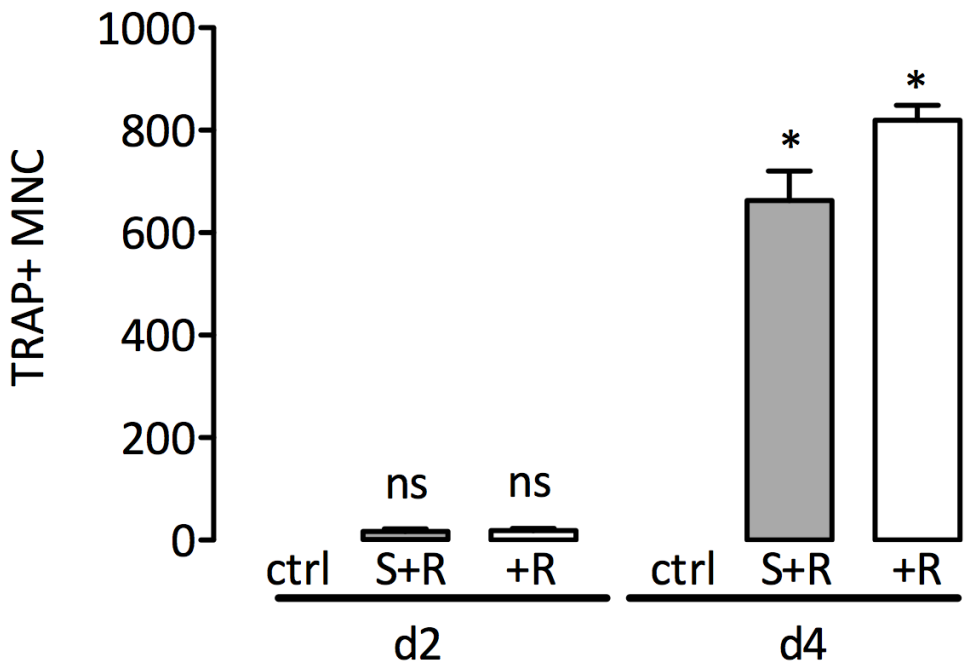

Figure 20: Quantification of TRAP positive multinuclear RAW 264.7 cells, the starvation group (S+R) and the group without serum starvation (+R). Both groups were supplemented with 7.5 ng/ml rmRANKL. TRAP positive cells with 3 or more nuclei were counted. The control group (ctrl) was cultured with standard

culture medium and showed no TRAP positive cells. Cells were fixed on days 2 and 4. ns $p>0.05$ and * $p\leq0.05$

Following these findings, we used the cell lysate from cells that underwent a 24-hour serum starvation. We examined SphK1 expression using gel electrophoresis with a 10 % acrylamide gel and western blot detection. In figure 21 the lysates from RAW 264.7 cells cultured with 7.5 ng/ml rmRANKL were compared to the cell lysate of RAW 264.7 cells without additional RANKL. The most intense bands could always be seen at 55 kDa and 43 kDa approximately, which corresponds with the suggested molecular weight from the datasheet (Santa Cruz Biotechnology sc-365401). The apparent increase in intensity when comparing day 4 to day 2 was not statistically significant ($p>0.05$) as the results varied between experiments.

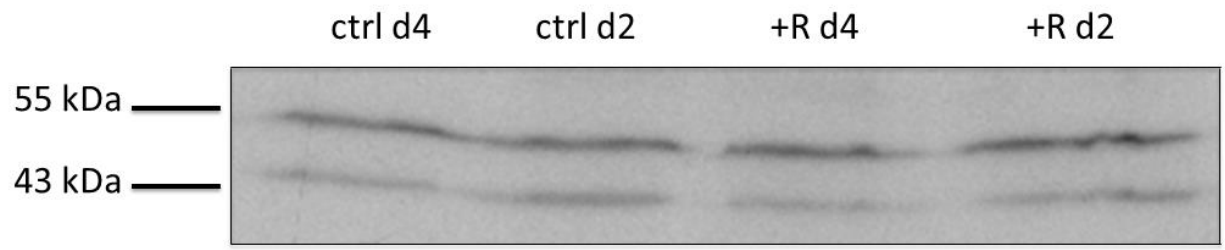

Figure 21: Detection of SphK1 in RAW 264.7 cell lysates using western blot. 75 µg of protein were loaded per lane and separated on a 10 % acrylamide gel. The control (ctrl) group is an undifferentiated RAW 264.7 cell lysate. +R group is a cell lysate from RAW 264.7 cells that were cultured with 7.5 ng/ml RANKL. All cells were starved for 24 hours before lysis on day 2 (d2) or 4 (d4). The SphK1 bands were found consistently at 43 kDa and 55 kDa.

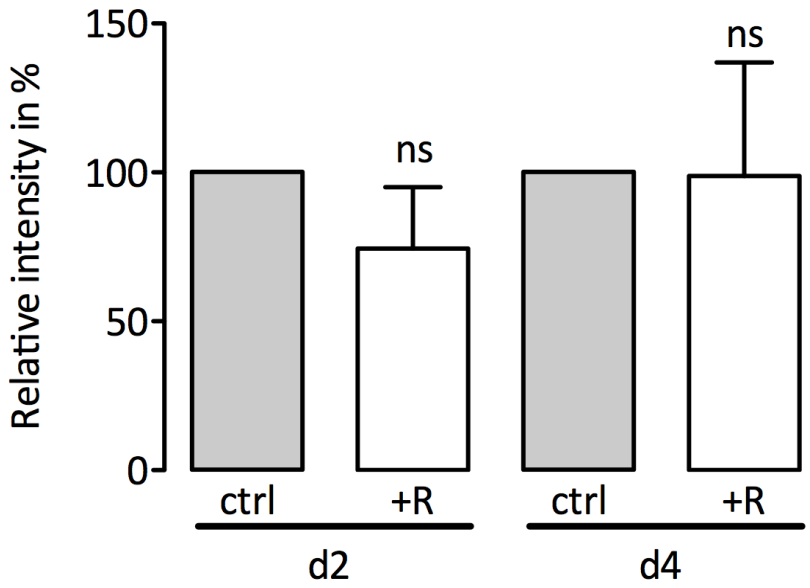

Figure 22: Quantification of SphK1 band intensity in RAW 264.7 cell lysates on day 2 and day 4. The ctrl group was cultivated with standard culture medium and the +R group was supplemented with 7.5 ng/ml rmRANKL. The intensity of the ctrl group was normalized to 100% for day 2 and day 4 and compared to the +R group. ns: $p>0.05$

4.3 Primary mouse osteoclast culture

As the results in the RAW 264.7 cell line did not support our hypothesis, we continued to test primary mouse osteoclasts. Since we had no data regarding serum starvation of primary mouse osteoclasts we first investigated the difference between a short-time serum starvation and a long-time serum starvation. All cells were cultured for 5 days in medium with 10 % serum and added rhM-CSF (30 ng/ml) and rmRANKL (30 ng/ml). Short starvation was 60 min of serum starvation; the cell morphology did not change much in comparison to the control. After 120 min of starvation the osteoclast membranes started to become permeable. 180 min starvation time showed advanced cell degradation, and the cell morphology changed drastically as can be seen in Figure 24. Based on these findings the serum starvation before the lysis was reduced to 60 min.

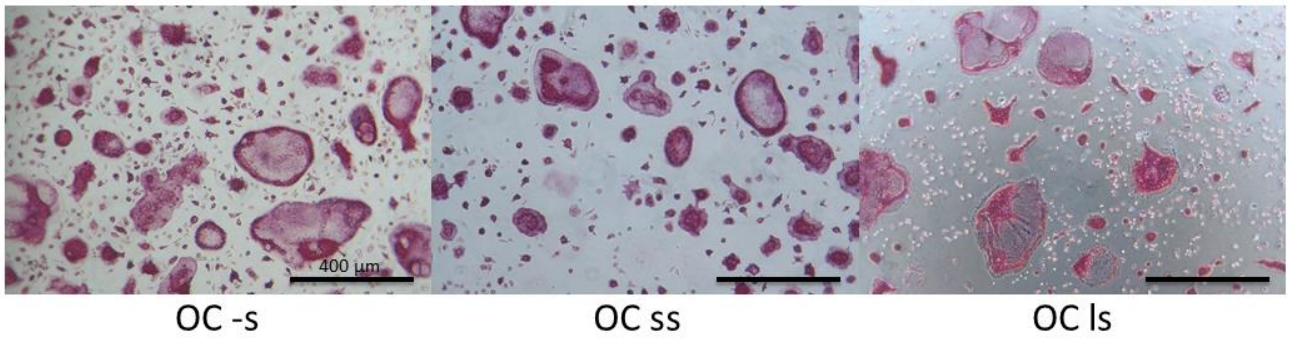

Figure 23: Effect of serum starvation on mouse bone marrow-derived osteoclasts. The (OC -s) group: no serum starvation, the (OC ss) group: starved for 60 min and the (OC ls) group was serum starved for 180 min. All groups were supplemented with rhM-CSF (30 ng/ml) and rmRANKL (30 ng/ml) supplementation, also during the starvation period.

To show that mature, multinucleated osteoclasts were present in the rmRANKL group only we stained all groups for TRAP. In figure 24 the difference between day 3 and day 5 is obvious, and the counting of TRAP positive mononuclear cells confirms this (figure 26). On day 3 no TRAP positive cells were present in either group, but the cells in the OC groups showed a slightly different morphology compared to the cells in the ctrl group. On day 5 multinucleated osteoclasts formed in the rmRANKL group (figure 25). Using the numbers from the counting TRAP positive cells we were also able to calculate the average number of osteoclasts in the rmRANKL supplemented group on day 5 (Table 6).

Table 6: Number of osteoclasts per cm² in a mouse bone marrow cell culture. The M-CSF group was cultured with 30 ng/ml rhM-CSF and the +RANKL group was cultured with 30 ng/ml rhM-CSF and 30 ng/ml rmRANKL. The numbers were obtained by counting TRAP positive cells:

Osteoclasts/ cm²	**+M-CSF**	**+M-CSF +RANKL**
day 3	0	0
day 5	0	2529

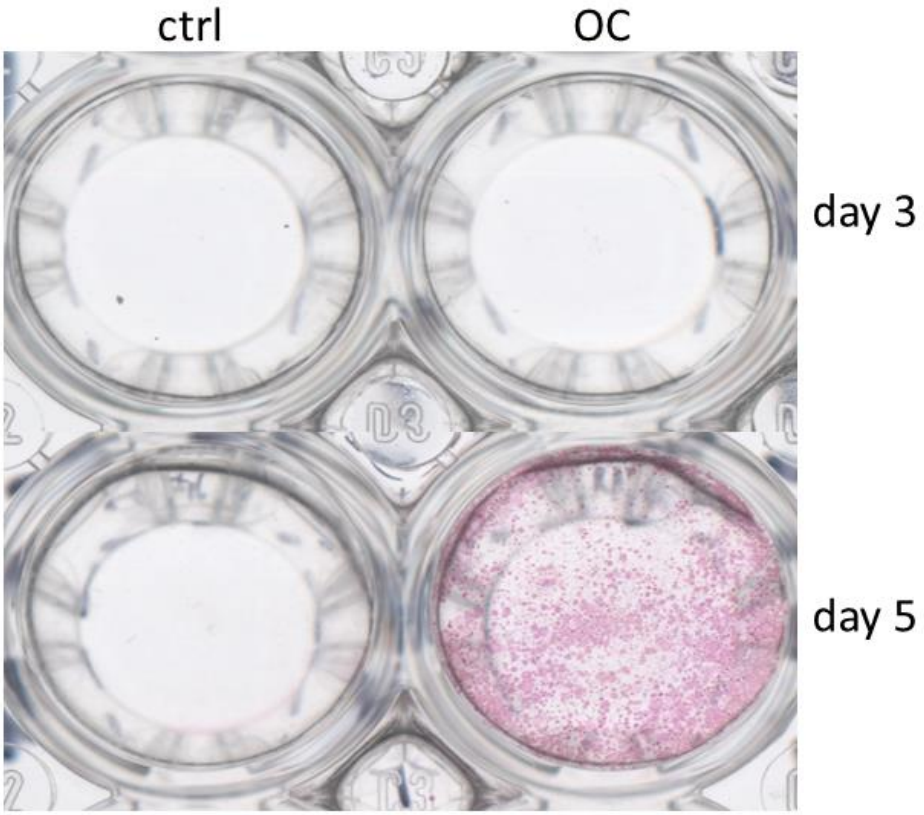

Figure 24: Osteoclast differentiation in mouse bone marrow cells with rhM-CSF and rmRANKL addition. TRAP staining was performed on days 3 and 5, corresponding to the time points of the cell lysis. The control group (ctrl) was treated with 30 ng/ml rhM-CSF, the osteoclast (OC) group was supplemented with rmRANKL (30 ng/ml) and rhM-CSF (30 ng/ml). TRAP positive cells are visible on day 5 in the OC group.

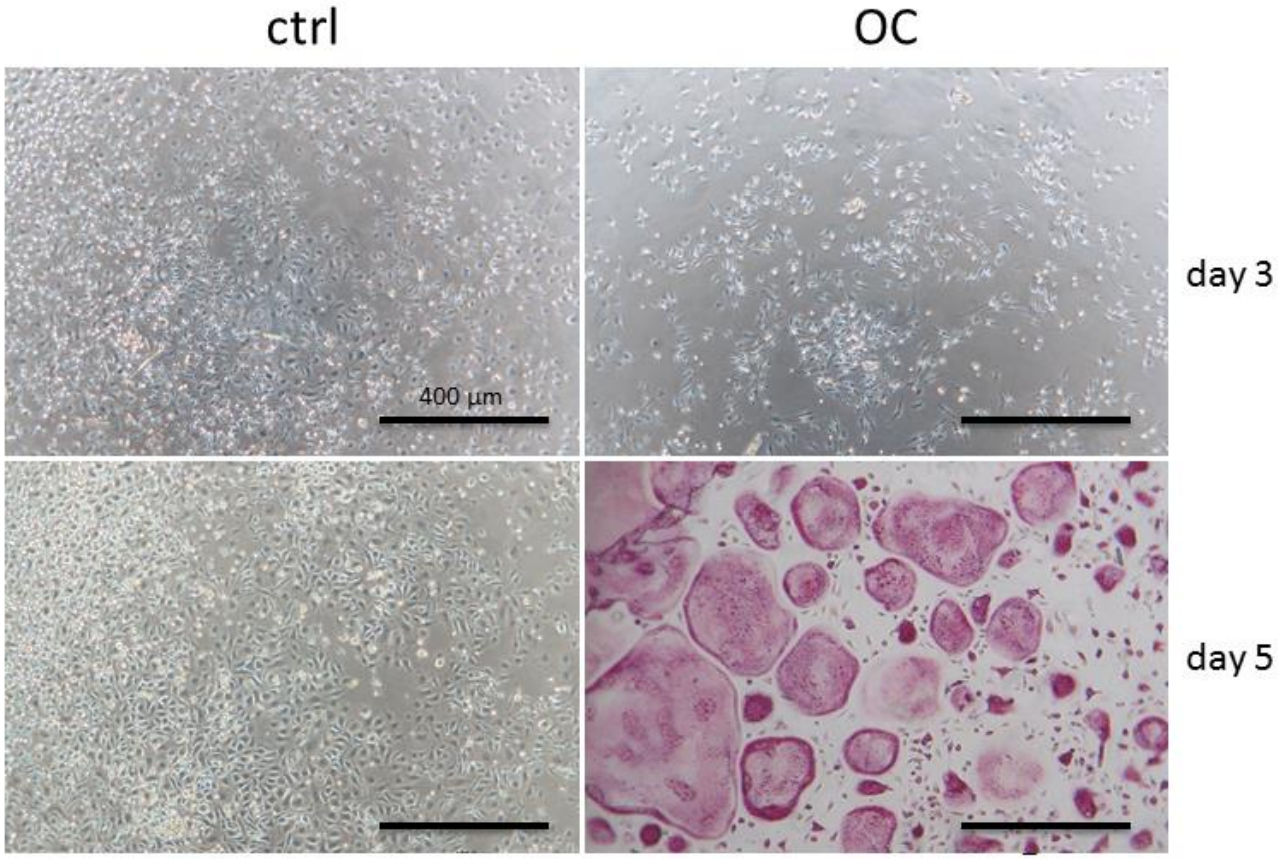

Figure 25: Osteoclast differentiation in mouse bone marrow cells with rmRANKL addition in 10x magnification. The ctrl group was cultured with 30 ng/ml rhM-CSF. The OC group was cultured with rhM-CSF (30 ng/ml) and rmRANKL (30 ng/ml). TRAP staining was done after fixation on days 3 and 5.

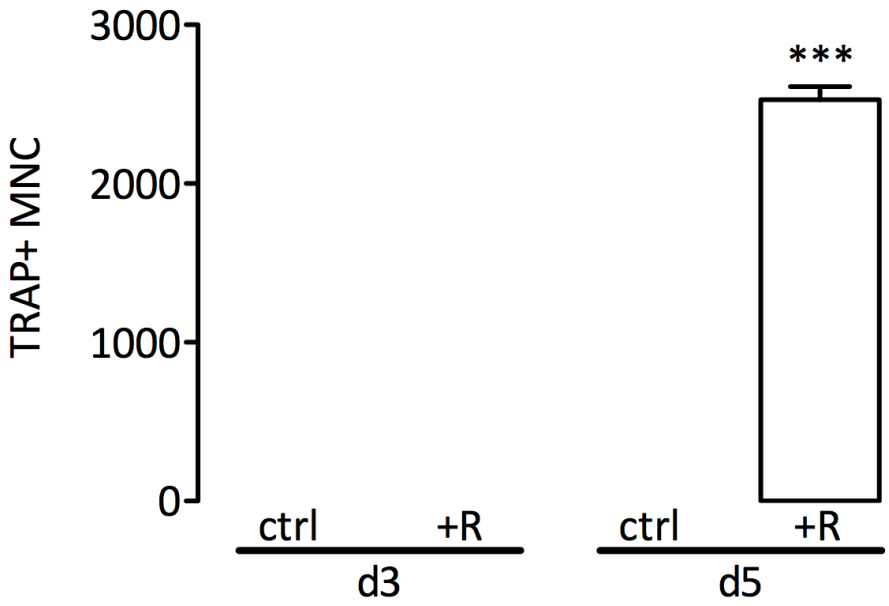

Figure 26: Time course of mouse bone marrow cell differentiation. TRAP positive cells with 3 or more nuclei were counted. ctrl groups: mouse bone marrow cells were cultured with 30 ng/ml rhM-CSF for 3 or 5 days. +R: mouse bone marrow cells cultured with rhM-CSF (30 ng/ml) and rmRANKL (30 ng/ml). ***: $p \leq 0.001$.

After western blotting with SphK1 antibody we saw a significant difference between days 3 and 5, but the difference in intensity between control and bone marrow cells treated with rmRANKL was not as pronounced (figure 27). Statistical analysis showed no significant difference due to the wide variation in the experiment (figure 28). The band with the highest intensity was found at 26 kDa. In some experiments the double band at 55 kDa and 43 kDa as seen in the RAW 264.7 cell lysate could also be found, but the band at 26 kDa was always present.

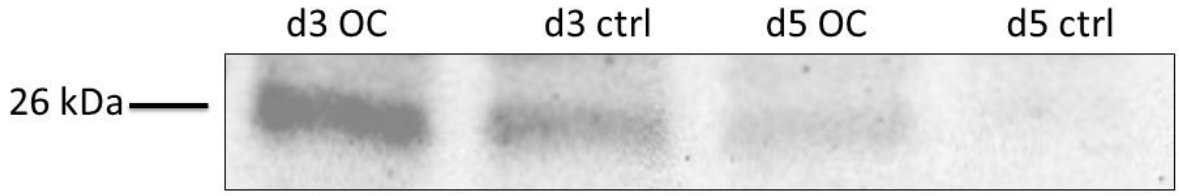

Figure 27: Detection of SphK1 in cell lysate from mouse bone marrow cell culture. 30 µg protein were loaded per lane and separated on a 10 % acrylamide gel. The OC group shows the cell lysate of BMM cells cultured with 30 ng/ml rhM-CSF and 30 ng/ml rmRANKL. The ctrl group is cell lysate from BMM cells cultured with 30 ng/ml rhM-CSF. Cells were lysed on days 3 and 5.

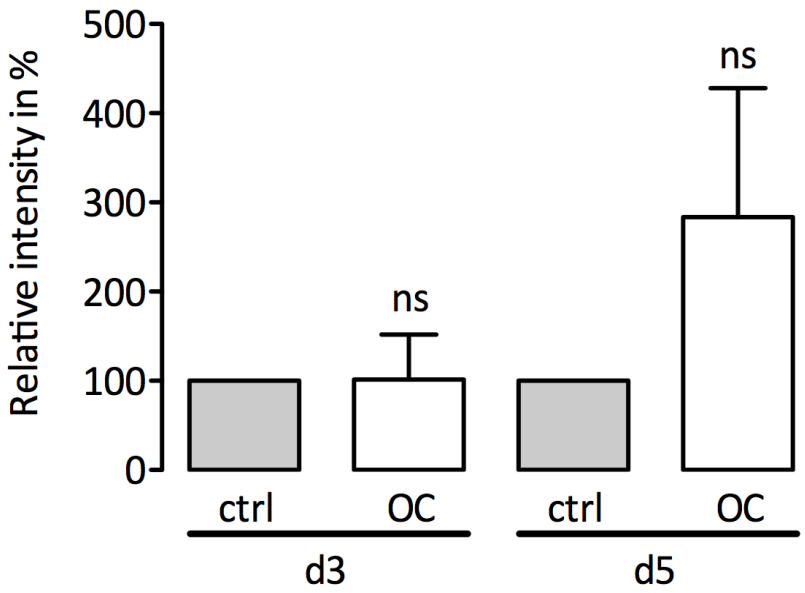

Figure 28: Quantification of SphK1 band intensity from mouse bone marrow cell lysate. The OC group was cultured with rhM-CSF (30 ng/ml) and rmRANKL (30 ng/ml). The ctrl group was cultured with 30 ng/ml rhM-CSF only. Cell lysates from day 3 and day 5 are shown. ns: $p>0.05$.

4.4 Osteoblast – osteoclast co-culture

According to Ryu, et al. 2006 it is possible that there are significant differences between single osteoclast culture and co-culture regarding SphK1 expression, so we also examined the expression in a mouse osteoblast-osteoclast co-culture. This culture method is less sensitive to serum starvation than the primary mouse osteoclast culture,

so we were able to do a serum starvation for 12 hours. In figure 29 the effect of serum starvation can be seen. Morphologically, the starved cells were slightly smaller. After counting the TRAP positive multinuclear cells, it was shown that the difference is not statistically significant ($p \leq 0.01$). For a better comparison we calculated the number of osteoclasts/cm² in the co-culture with and without starvation and the control osteoblast culture. Table 7 shows that in the starvation group the osteoclast density on day 5 is slightly lower than in the group without starvation.

Table 7: Comparison of single mouse osteoblast culture to osteoblast-osteoclast co-culture and an osteoblast-osteoclast co-culture subjected to 12-hour serum starvation, presented as number of osteoclasts per cm^2 after TRAP staining of cultures:

Osteoclasts/cm²	**osteoblast group**	**co-culture group**	**co-culture with starvation**
day 1	0	0	0
day 3	0	317	211
day 5	1	1276	1146

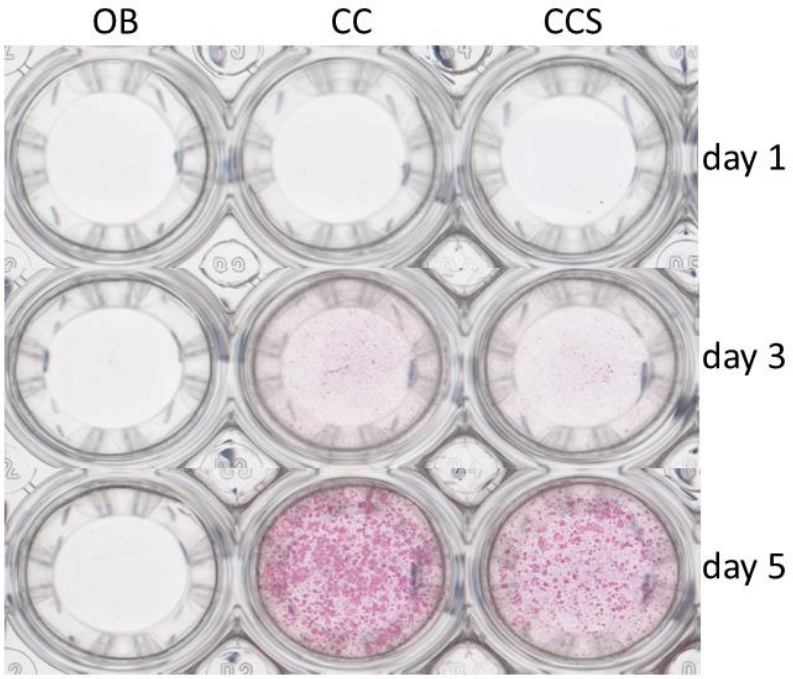

Figure 29: The effect of serum starvation on osteoclast differentiation in co-culture. The cells were stained for TRAP on days 1, 3 and 5. A single osteoblast culture (OB) is shown in the leftmost column, cultured with 10 µM 1,25-dihydroxyvitamin D_3 and 1 mM Prostaglandin E_2. CC shows a co-culture without serum starvation which was cultured with 10 µM 1,25-dihydroxyvitamin D_3 and 1 mM Prostaglandin E_2. The rightmost column shows a co-culture supplemented with 10 µM 1,25-dihydroxyvitamin D_3 and 1 mM Prostaglandin E_2 that was serum starved for 12 hours (CCS).

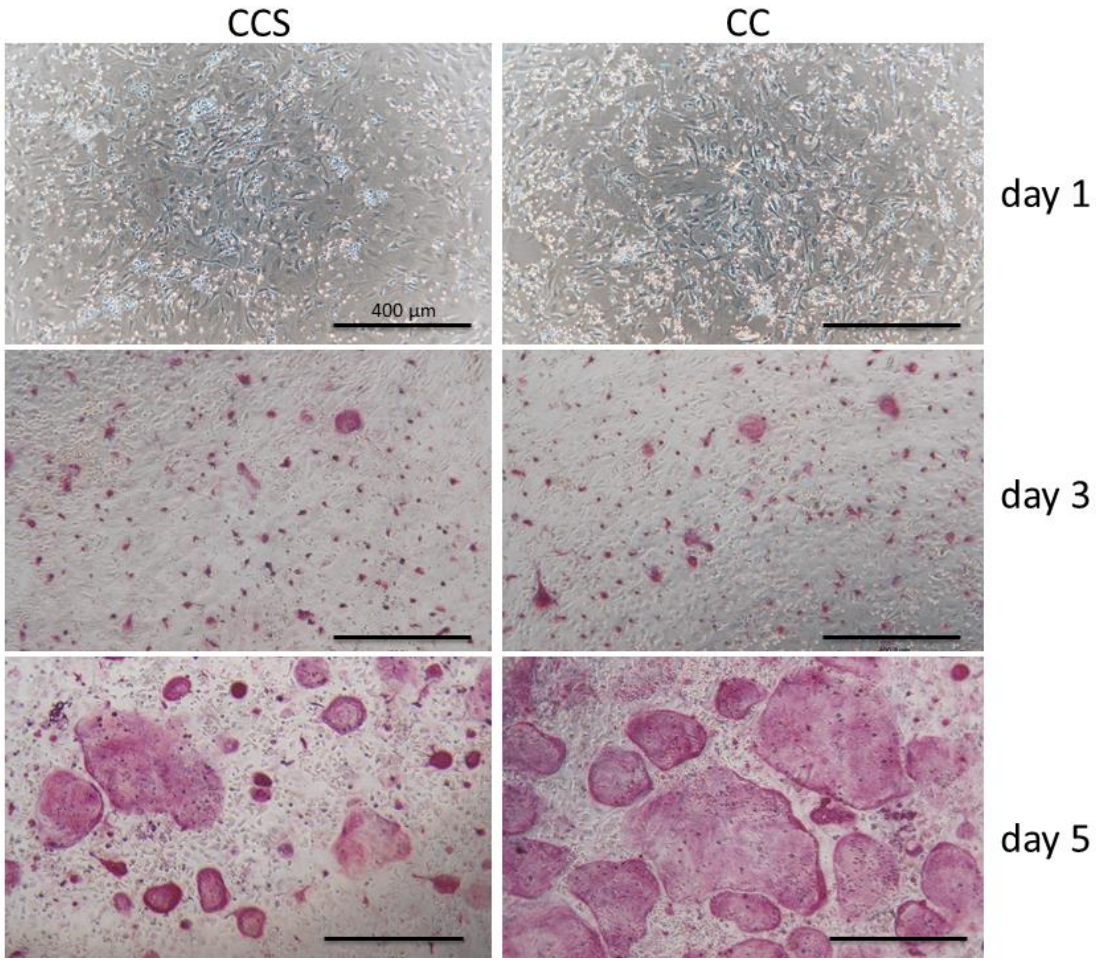

Figure 30: Osteoclast differentiation in co-culture under the effect of serum starvation. A 10x magnification was used to observe the cell morphology. Left column: a co-culture that was serum starved for 12 hours is shown (CCS). Right column: a co-culture (CC) without serum starvation. TRAP staining was done on days 1, 3 and 5.

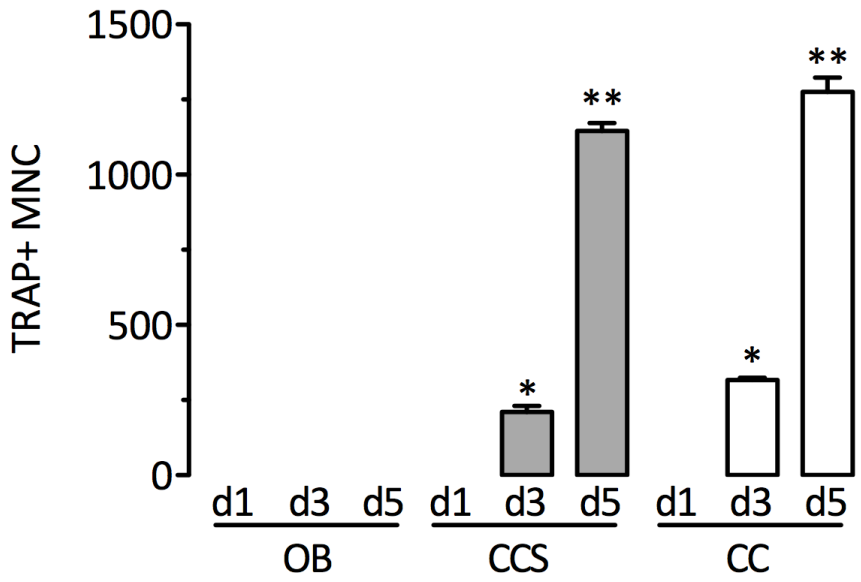

Figure 31: Enumeration of TRAP positive multinuclear cells in single mouse osteoblast culture and osteoblast-osteoclast co-culture under the influence of serum starvation. TRAP positive cells with three or more nuclei were counted. OB shows the single osteoblast cultures. CCS shows osteoblast-osteoclast co-cultures which were subjected to 12-hour serum starvation. The CC group is an osteoclast-osteoblast co-culture without starvation. Cells were stained on days 1, 3 and 5. *: $p \leq 0.05$; **: $p \leq 0.01$.

The co-cultures were serum starved for 12 hours before lysis. The blots from the osteoclast cell lysate showed one significant band at around 26 kDa (Figure 32). The expected double band at 55 kDa and 43 kDa, which was always present in the RAW 264.7 cell lysates, was not visible. As control group we chose a single mouse osteoblast culture. Here SphK1 was also present, but at much lower concentrations (Figure 32). We found no significant difference between the intensity of the bands from days 1, 3 and 5 in the co-culture or the osteoblast culture (Figure 33).

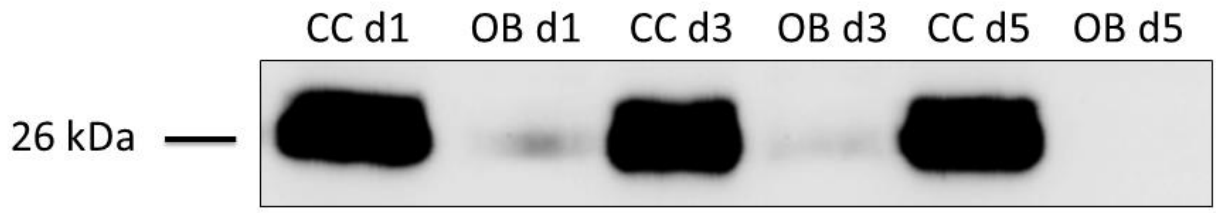

Figure 32: Detection of SphK1 in cell lysate from mouse osteoblasts (OB) and osteoclast- osteoblast co-culture (CC). 40 µg protein were separated on a 10 % acrylamide gel. The cell lysates from day 1, 3 and 5 are shown.

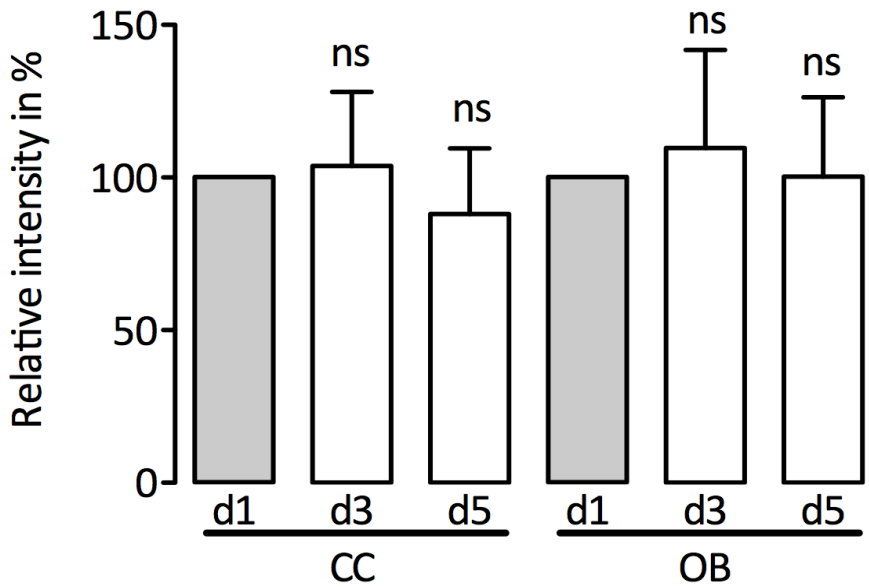

Figure 33: Quantification of SphK1 band intensity in co-culture and osteoblasts. CC shows the band intensity of osteoclast-osteoblast co-cultures on days 1, 3 and 5 normalized to the intensity of the CC band on day 1. OB shows the band intensity of single osteoblast cultures on days 1, 3 and 5. The absolute band intensity here was normalized to day 1 of the OB band. ns vs. d1 band

When we compared the cell lysates of two different experiments we saw that the difference between them was bigger than the difference between the days 1 to 5 in one single experiment. In figure 33 and 34 we compared the relative intensity normalized to day 1. We also looked at the absolute intensity (data not shown), the amount of OB

intensity was almost not visible. There was no statistical significance between the co-culture groups (Figure 34).

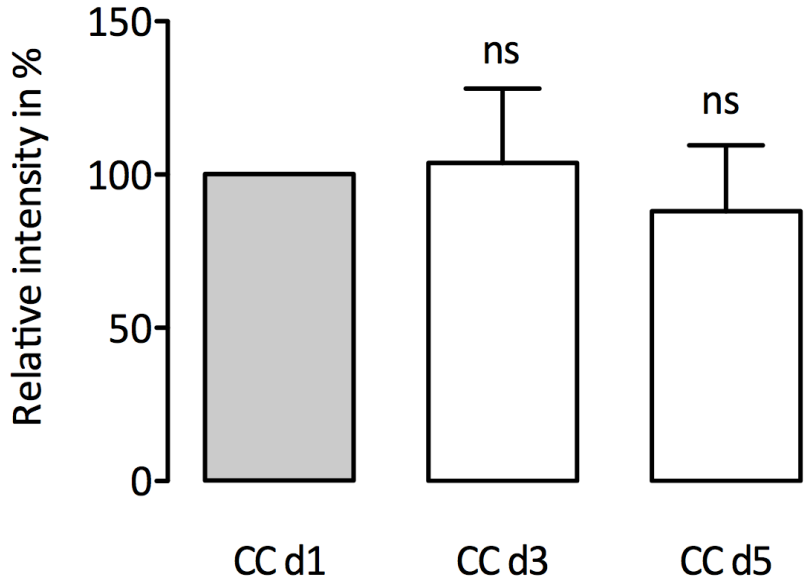

Figure 34: Quantification of SphK1 band intensity in osteoclast-osteoblast co-culture (CC). The relative intensity of the bands from co-culture cell lysate comparing days 1, 3 and 5. ns vs CC d1 .

The statistical analysis was done with a 1-way ANOVA and Tukey's post-hoc test for all experiments. Total protein staining was done using a Ponceau S solution which was then scanned and analysed with the ChemiDoc™ system from BioRad®.

4.5 Summary

To summarize, we found a new band in the western blot from the mouse osteoclast cell lysate at 26 kDa, which was not visible in the RAW 264.7 cell lysate. The bands that are located at 55 kDa and 43 kDa were faintly visible in the primary osteoclast cell culture in contrast to the RAW 264.7 cell lysate. Nevertheless, the intensity of the band at 26 kDa did not change significantly during the osteoclastogenesis. The newly found band

represents a significant difference between the two culture systems, and we inquired if this was due to the RAW 264.7 cells being a cell line or an osteoclast specific phenomenon.

Therefore, we tested an osteoblast-osteoclast co-culture and compared it to a single osteoblast culture. According to the results from the counting of TRAP positive cells a 12-hour serum starvation did not have a big effect on the number of mature osteoclasts in the culture. We decided to starve them overnight before the lysis as we have done with the RAW 264.7 cells.

In the osteoblast lysate the band at 26 kDa could not be seen, but in the co-culture lysate it was clearly present. The two bands at 55 kDa and 43 kDa were sometimes also present. We concluded from this that the band at 26 kDa seems to be relatively specific for mouse bone marrow-derived osteoclasts and their precursors. It is already present on day 1 in the co-culture and the undifferentiated, rhM-CSF supplemented mouse bone marrow cells, but very faint at most in the single osteoblast culture. As shown in table 6, the cells from neonatal mouse calvariae are also able to differentiate into osteoclasts while PGE_2 and 1,25-dihydroxyvitamin D_3 are present, but in very low quantities.

5. Discussion

During this diploma thesis I tried to find evidence that the expression of SphK1 in osteoclasts changes during their evolution. The first researchers to propose the increase of SphK1 expression during osteoclastogenesis were (Ryu, et al. 2006). Another publication from Pederson, et al. 2008 was able to confirm some of these findings. To test this hypothesis, I used single and co-cultures of osteoclast and osteoblast precursor cells and tried to detect the changes in protein expression using a Western Blot system.

I found that a 60-minute incubation time with RIPA cell lysis buffer supplemented with a protein inhibitor cocktail not only increased the total protein yield from the cell lysate but also showed more intense bands from SphK1 than a shorter incubation time. Following these findings, I decided to treat all cell lysates using this lysis buffer with a 60-minute incubation time. The cells were cultured as described in the 'Results'. I first used RAW 264.7 cells because of their fast growth and to assure the detection capabilities of the SphK1 antibody. In contrast to the datasheet (Santa Cruz Biotechnology sc-365401) and the findings of Pederson, et al. 2008 I always saw two bands around the proposed molecular weight instead of the one single band. I speculate that they are SphK1, since Vu, et al. 2017 found similar bands in the lysate from red blood cells, and I was able to repeat these findings in several blots. Another group around Kihara also showed a double band when detecting SphK1 in cell lysates (Kihara, et al. 2006). Vu and his colleagues also used RIPA buffer, whereas the group around Pederson used a different lysis buffer. As I supplemented protease inhibitors it might be that I conserved the different isoforms. I tried to compensate that by combining the intensity of the two bands. After adjusting the absolute intensity for the loading control, I compared the change in intensity in percent. Statistical analysis confirmed my initial impressions that the difference in expression during osteoclastogenesis was not significant.

To confirm the results obtained in the RAW 264.7 cell line I then decided to use primary mouse cells to investigate the SphK1 expression. First, the osteoclast culture from mouse bone marrow precursor cells had to be optimized and tested for its response under serum starvation conditions. Mature osteoclasts starved for 60 min showed almost no difference to the control group without serum starvation. In contrast,

observation of longer starvation periods showed that after 120 min the cell membranes started to become permeable and after 180 min in almost all osteoclasts the membranes started to break down. So, we can conclude that osteoclasts from mouse bone marrow precursor cells are able to withstand a short serum starvation of up to 60 min. The cultures used for the western blots were then treated this way.

My results show that the bands located at 55 kDa and 43 kDa that were consistently visible in the RAW 264.7 cell lysate were not as intense in the osteoclast cell lysate. Additionally, there was a new band visible at 26 kDa with a significantly higher intensity. Statistical analysis comparing the intensity over time of the new band in the osteoclast culture showed no significant increase in the band at 26 kDa.

This finding confirmed that the osteoclastogenesis does not seem to lead to an increased SphK1 expression. But a new question came up as to the meaning of the new band at 26 kDa. To find out if this suspected difference in isoforms was a phenomenon of primary single mouse osteoclast cells or if this was because RAW 264.7 cells are a cell line with different properties than primary cells, I tested primary mouse osteoblasts and a co-culture of osteoblasts and osteoclasts.

These cells were also subjected to a serum starvation period. According to the results from the enumeration of TRAP positive cells, a 12-hour serum starvation did not have a big impact on the number of mature osteoclasts.

The lysate from the co-culture also showed an intensive band at 26 kDa, in contrast to the osteoblast lysate. In both lysates bands at 55 kDa and 43 kDa were at least faintly visible, in the osteoblast lysate they seemed more intense than in the co-culture. According to statistical analysis of the change in intensity of the band at 26 kDa the difference between the groups was not significant.

Following these results, I conclude that the hypothesis of an increase in SphK1 expression during osteoclastogenesis could not be supported in our experiments. The following paragraphs will be discussing possibilities causing these differences and possible future experiments.

Looking at the methods of the other groups, I changed some parameters. Pederson, et al. 2008 did not subject their cells to a serum starvation prior to the lysis, neither did the group around Ryu, et al. 2006. This could have led to a different protein expression pattern, as starvation conditions are stressful for the cells. Another difference in experimental procedures was the lysis itself. I supplemented the RIPA buffer with a protease inhibitor cocktail in contrast to the other groups. This, as mentioned before, could have conserved different isoforms. SphK1b seems to exhibit abnormal mobility on SDS-PAGE and is also very unstable in contrast to the SphK1a isoform (Kihara, et al. 2006). Addition of protease inhibitors could have conserved this isoform and lead to a different result than a cell lysis without supplemented inhibitors.

Another difference was the antibody used. Since the SphK1 antibodies other groups used were no longer available, I decided on the monoclonal SphK1 antibody from Santa Cruz Biotechnology Inc. (sc-365401). The double band I saw in the RAW 264.7 lysate was not pictured in the datasheet or the results from the aforementioned groups, but in the publications of Ji, et al. 2015 and Vu, et al. 2017 two SphK1 bands at approximately the same molecular weight as I found can also be seen. Other groups also found SphK1 at a molecular weight of ±43 kDa (Guo, et al. 2016, Shao, et al. 2015) but only showed one band, most publications do not indicate the molecular weight at which the SphK1 band was found (Kim, et al. 2015, Pederson, et al. 2008, Ryu, et al. 2006, Schiefler, et al. 2014, Song, et al. 2011). One possible explanation for the two SphK1 bands could be that the monoclonal SphK1 antibodies show more bands than the polyclonal SphK1 antibodies. Comparing two datasheets from Cell Signaling Technology®, the polyclonal SphK1 antibody (Cell Signaling Technology #3297) shows fewer bands in the sample cell lysates than the monoclonal SphK1 antibody (Cell Signaling Technology #12071). In both datasheets different immortalised cell lines were used as examples, but not from the same cell lines. This makes the datasheets only partially comparable.

The oncogenic role of sphingosine kinase was investigated by Xia, et al. 2000, and showed that the overexpression of SphK in cells led to colony growth in soft agar and tumour formation in mice. These oncogenic properties fit with the fact that immortalised cell lines are often used as a positive control for SphK1 antibodies. RAW

264.7 cells were also listed as a positive control in the Santa Cruz Biotechnology® datasheet (Santa Cruz Biotechnology sc-365401).

The difference between the RAW 264.7 cell lysates and the primary mouse osteoclast cell lysates could be based on the difference in protein expression between primary mouse cells and RAW 264.7 cells. In the work of Chamberlain, et al. 2009 the difference in expression of some cytokines between RAW 264.7 macrophages and two other frequently used murine macrophage cell lines and primary murine bone marrow macrophages are compared. Since we saw a difference between RAW 264.7 cell lysates and primary mouse osteoclast lysates regarding the band at 26 kDa we hypothesized that the expression of the SphK1 isoforms might be different in the RAW 264.7 cell line and the primary mouse osteoclast cells. As all cells were lysed according to the same protocol the different isoforms should not be due to the protease inhibition. The fact that the SphK1 expression in RAW 264.7 cells looks more like the primary mouse osteoblast cells than the primary mouse osteoclasts suggests that the RAW 264.7 cells might not be a suitable model to study SphK1 expression in osteoclasts.

Results from Xia, et al. 2000 suggest that the increased activation of SphK1 is more important for high S1P levels than an increased expression of the protease itself. These findings would support our results that the expression does not change significantly during osteoclastogenesis. Most of the recent publications focus on the SphK1 expression on a genetic level or the influence of S1P itself on bone cells (Shiwaku, et al. 2015,Keller, et al. 2014,Kikuta, et al. 2013). Taken together it appears that the expression of SphK1 on a genetic and protein level is not directly correlated with the S1P levels in the cells. The activation of SphK1 seems to be more crucial for the cellular communication.

The hypothesis that S1P is an important cytokine for bone remodelling is supported by the work of Ishii and his colleagues. In two publications they looked at the motility of osteoclast precursor cells using RAW 264.7 cells (Ishii, et al. 2009, Ishii, et al. 2010). These cells express the S1PR1, which is a specific S1P receptor located on the cell membrane that reacts to different S1P concentrations. High S1P concentration gradients as are present between the blood stream and the bone surface can induce migration of

the osteoclast precursor cells. Concentrations of $1x10^{-8}$ M S1P prompted the osteoclast precursor cells to move towards the S1P. In conclusion, the difference in S1P concentration between blood and the bone surface is important for osteoclast precursors to be able to migrate from the circulating blood to the bone surface where they can undergo cell fusion to form mature osteoclasts.

Taken together these results show that future work is required to support the new hypothesis that the SphK1 expression does not change during osteoclastogenesis. A more sensitive method to detect more subtle changes in protein expression could be suitable to show a difference between osteoclast precursors and mature osteoclasts. In case that these differences are only small, the question arises if SphK1 is in fact as important for signalling molecule in the osteoclast-osteoblast communication as described in the previous literature. Other experiments could focus on the S1P expression in osteoclasts and their precursors as well as the difference to osteoblasts or the correlation of S1P concentration in the supernatant of primary mouse osteoblast and osteoclast cultures to the expression of SphK1.

6. Conclusion

Bone remodeling relies on a complex communication between osteoblastic and osteoclastic cell lines. Soluble and membrane bound factors as well as signaling molecules embedded in the bone matrix work together to enable continuous remodeling to ensure healthy bone structure. One potential clastokine is sphingosine-1-phosphate. This lipid-signaling molecule is found ubiquitously in the body. Some groups hypothesized its role as an osteoclast specific signal and found SphK1 to be important in the signaling pathway. Our hypothesis was based on these findings, and we wanted to look at the SphK1 expression in different cell types. Optimizing each culture model to obtain mature osteoclasts on day 4 or 5 we used cell lysis involving protein inhibitors to prepare for western blots. Interestingly, we found SphK1 in all cell lines but no significant difference in intensity during osteoclastogenesis. The biggest change in the protein pattern was an unexpected band at a lower molecular weight (26 kDa) in the single mouse osteoclast culture and the osteoblast-osteoclast co-culture. Since others have researched the abnormal mobility of SphK1 isoforms in western blot we were certain to have found the right protein, as they also showed a band at this molecular weight. In the RAW 264.7 cell culture and the primary mouse osteoblast culture we only saw bands at 43 kDa. A second band at 55 kDa was also visible, and to correct for the different isozymes we added the densities of the two bands together when calculating the intensity for the RAW 264.7 cell culture. In the other culture models we focused on the more intense band at 26 kDa. All osteoclast cultures showed mature, multinucleated osteoclasts on day 4 and 5 and were repeated to ensure statistically relevant results. Our results show that the protein bands obtained from the mouse osteoclasts seem to differ from RAW 264.7 cells. There are several possibilities why the hypothesis could not be supported with the conducted experiments. The difference in SphK1 antibody, the use of protease inhibitors, the starvation period before cell lysis and western blotting being a suboptimal detection method for this particular protein. More research needs to be done to look more closely at the SphK1 expression in osteoclasts and its relation to the S1P secretion.

7. Abstract

Osteoclast-osteoblast communication works through different channels, one of those are the cytokines. Cytokines secreted by osteoclasts are also called ‘clastokines’ and they are not as well researched yet as well as the cytokines secreted by osteoblasts.

One suspected clastokine is sphingosine-1-phosphate. This molecule was found to enhance mineralization in osteoblasts. Some researchers found an increase in Sphk1, which is one of the enzymes responsible for phosphorylation of sphingosine into sphingosine-1-phosphate during osteoclastogenesis.

Based on this premise we prepared cell lysates from single cell culture of RAW 264.7 cells as well as lysates from single and co-culture of primary mouse osteoblast and osteoclast precursors at different time points after RANKL addition and separated them using gel electrophoresis. Using western blot detection, we were unable to find an increase of SphK1 during osteoclastogenesis.

What we could see were different isoforms of SphK1 in RAW 264.7 cells and primary mouse osteoblasts versus primary mouse osteoclasts. In the mouse osteoclasts an additional isoform was visible, which we could only see very faintly in the mouse osteoblasts and RAW 264.7 cells.

Further research is needed to confirm these findings, using more sensitive detection methods and additional examination of sphingosine-1-phosphate in the supernatant.

8. Zusammenfassung

Die Kommunikation zwischen Osteoblasten und Osteoklasten läuft über verschiedene Kanäle, zum Beispiel über die Zytokine. Spezielle Zytokine, die von Osteoklasten sekretiert werden, werden auch „Klastokine" genannt. Diese sind noch nicht so gut erforscht wie die von Osteoblasten sekretierten Zytokine.

Ein vermutetes Klastokin ist Sphingosin-1-Phosphat. Man hat herausgefunden, dass dieses Molekül die Mineralisation von Osteoblasten fördert. Einige Forscher haben einen Anstieg an SphK1 während der Osteoklastogenese festgestellt. SphK1 ist eines der Enzyme, das für die Phosphorylierung von Sphingosin zu Sphingosin-1-Phosphat verantwortlich ist.

Basierend auf diesen Hypothesen verwendeten wir Zelllysate von RAW 264.7-Zellkulturen und Zelllysate von Einzel- und Co-Kulturen primärer Maus-Osteoblasten und -Osteoklastenvorstufen zu verschiedenen Zeitpunkten nach der Zugabe von RANKL. Die Zelllysate wurden mittels Gelelektrophorese aufgetrennt und die SphK1 mit Western-Blots detektiert. Wir konnten dabei keinen signifikanten Anstieg während der Osteoklastogenese beobachten.

Allerdings entdeckten wir einen Unterschied im Western Blot von RAW 264.7-Zellen und primären Maus-Osteoblasten gegenüber primären Maus-Osteoklasten. In den Osteoklasten war eine zusätzliche Isoform sichtbar, die in RAW 264.7-Zellen und Osteoblasten höchstens sehr schwach ausgeprägt war.

Weitere Untersuchungen mit sensibleren Methoden sind notwendig, um die vorliegenden Ergebnisse zu bestätigen. Auch sollten Untersuchungen im Überstand der Zellkulturen auf S1P durchgeführt werden, um genauere Ergebnisse über die Entwicklung während der Osteoklastogenese zu erhalten.

9. Literature

Albrecht KF, Hornbostel H. Innere Medizin in Praxis und Klinik. 2., überarb. u. erw. Aufl. ed. Albrecht KF, Hornbostel H, editors. Stuttgart [u.a.]: Thieme; 1978. Getr. Zählung p.

Arboleya L, Castañeda S. Osteoinmunología: el estudio de la relación entre el sistema inmune y el tejido óseo. Reumatol Clin. 2013;9(5):303-15.

Billich A, Bornancin F, Devay P, Mechtcheriakova D, Urtz N, Baumruker T. Phosphorylation of the immunomodulatory drug FTY720 by sphingosine kinases. J Biol Chem. Nov 28 2003;278(48):47408-15. Epub 2003/09/18.

Bonewald LF. The amazing osteocyte. J Bone Miner Res. Feb 2011;26(2):229-38. Epub 2011/01/22.

Boyle WJ, Simonet WS, Lacey DL. Osteoclast differentiation and activation. Nature. 2003;423(6937):337-42.

Cell Signaling Technology. SPHK1 (D1H1L) Rabbit mAb https://media.cellsignal.com/pdf/12071.pdf?__hstc=157313765.853d8ec6e305616e5997c65fddb409b1.1513006608574.1535616855945.1537427915819.4&__hssc=157313765.1.1537427915819&__hsfp=3712334065#_ga=2.146448055.2035507085.1537427912-1424985003.1513006606 October 9, 2018

Cell Signaling Technology. SPHK1 Antibody https://media.cellsignal.com/pdf/3297.pdf?__hstc=157313765.853d8ec6e305616e5997c65fddb409b1.1513006608574.1535616855945.1537427915819.4&__hssc=157313765.2.1537427915819&__hsfp=3712334065#_ga=2.132397965.2035507085.1537427912-1424985003.1513006606 October 9, 2018

Chamberlain LM, Godek ML, Gonzalez-Juarrero M, Grainger DW. Phenotypic non-equivalence of murine (monocyte-) macrophage cells in biomaterial and inflammatory models. J Biomed Mater Res A. Mar 15 2009;88(4):858-71. Epub 2008/03/22.

Charles JF, Aliprantis AO. Osteoclasts: more than 'bone eaters'. Trends Mol Med. Aug 2014;20(8):449-59. Epub 2014/07/11.

Chen G, Deng C, Li YP. TGF-beta and BMP signaling in osteoblast differentiation and bone formation. Int J Biol Sci. 2012;8(2):272-88. Epub 2012/02/03.

Clarke B. Normal bone anatomy and physiology. Clin J Am Soc Nephrol. Nov 2008;3 Suppl 3:S131-9. Epub 2008/11/15.

Everts V, Delaisse JM, Korper W, Jansen DC, Tigchelaar-Gutter W, Saftig P, et al. The Bone Lining Cell: Its Role in Cleaning Howship's Lacunae and Initiating Bone Formation. J Bone Miner Res. 2002;17(1):77-90.

Florencio-Silva R, Sasso GR, Sasso-Cerri E, Simoes MJ, Cerri PS. Biology of Bone Tissue: Structure, Function, and Factors That Influence Bone Cells. Biomed Res Int. 2015;2015:421746. Epub 2015/08/08.

Grigoriadis AE. Differentiation of muscle, fat, cartilage, and bone from progenitor cells present in a bone-derived clonal cell population: effect of dexamethasone. The Journal of Cell Biology. 1988;106(6):2139-51.

Guntur AR, Rosen CJ. Bone as an endocrine organ. Endocr Pract. Sep-Oct 2012;18(5):758-62. Epub 2012/07/13.

Guo S, Xie Y, Fan JB, Ji F, Wang S, Fei H. alpha-Melanocyte stimulating hormone attenuates dexamethasone-induced osteoblast damages through activating melanocortin receptor 4-SphK1 signaling. Biochem Biophys Res Commun. Jan 8 2016;469(2):281-7. Epub 2015/12/04.

Heilmann A, Schinke T, Bindl R, Wehner T, Rapp A, Haffner-Luntzer M, et al. Systemic treatment with the sphingosine-1-phosphate analog FTY720 does not improve fracture healing in mice. J Orthop Res. Nov 2013;31(11):1845-50. Epub 2013/07/03.

Ishii M, Egen JG, Klauschen F, Meier-Schellersheim M, Saeki Y, Vacher J, et al. Sphingosine-1-phosphate mobilizes osteoclast precursors and regulates bone homeostasis. Nature. Mar 26 2009;458(7237):524-8. Epub 2009/02/11.

Ishii M, Kikuta J, Shimazu Y, Meier-Schellersheim M, Germain RN. Chemorepulsion by blood S1P regulates osteoclast precursor mobilization and bone remodeling in vivo. J Exp Med. Dec 20 2010;207(13):2793-8. Epub 2010/12/08.

Ji F, Mao L, Liu Y, Cao X, Xie Y, Wang S, et al. K6PC-5, a novel sphingosine kinase 1 (SphK1) activator, alleviates dexamethasone-induced damages to osteoblasts through activating SphK1-Akt signaling. Biochem Biophys Res Commun. Mar 13 2015;458(3):568-75. Epub 2015/02/15.

Keller J, Catala-Lehnen P, Huebner AK, Jeschke A, Heckt T, Lueth A, et al. Calcitonin controls bone formation by inhibiting the release of sphingosine 1-phosphate from osteoclasts. Nat Commun. Oct 21 2014;5:5215. Epub 2014/10/22.

Kihara A, Anada Y, Igarashi Y. Mouse sphingosine kinase isoforms SPHK1a and SPHK1b differ in enzymatic traits including stability, localization, modification, and oligomerization. J Biol Chem. Feb 17 2006;281(7):4532-9. Epub 2005/12/22.

Kikuta J, Kawamura S, Okiji F, Shirazaki M, Sakai S, Saito H, et al. Sphingosine-1-phosphate-mediated osteoclast precursor monocyte migration is a critical point of control in antibone-resorptive action of active vitamin D. Proc Natl Acad Sci U S A. April 23, 2013 2013;110(17):7009-13.

Kim HS, Yoon G, Ryu JY, Cho YJ, Choi JJ, Lee YY, et al. Sphingosine kinase 1 is a reliable prognostic factor and a novel therapeutic target for uterine cervical cancer. Oncotarget. 2015;6(29):26746-56.

Kogianni G, Mann V, Noble BS. Apoptotic bodies convey activity capable of initiating osteoclastogenesis and localized bone destruction. J Bone Miner Res. Jun 2008;23(6):915-27. Epub 2008/04/26.

Lotinun S, Kiviranta R, Matsubara T, Alzate JA, Neff L, Luth A, et al. Osteoclast-specific cathepsin K deletion stimulates S1P-dependent bone formation. J Clin Invest. Feb 2013;123(2):666-81. Epub 2013/01/17.

Mizugishi K, Yamashita T, Olivera A, Miller GF, Spiegel S, Proia RL. Essential role for sphingosine kinases in neural and vascular development. Mol Cell Biol. Dec 2005;25(24):11113-21. Epub 2005/11/30.

Nakamura I, Takahashi N, Jimi E, Udagawa N, Suda T. Regulation of osteoclast function. Mod Rheumatol. Apr 2012;22(2):167-77. Epub 2011/09/29.

Pederson L, Ruan M, Westendorf JJ, Khosla S, Oursler MJ. Regulation of bone formation by osteoclasts involves Wnt/BMP signaling and the chemokine sphingosine-1-phosphate. Proc Natl Acad Sci U S A. 2008;105(52):20764-9.

Pitson SM. Regulation of sphingosine kinase and sphingolipid signaling. Trends Biochem Sci. Feb 2011;36(2):97-107. Epub 2010/09/28.

Pyne S, Pyne NJ. Sphihngosine 1-phosphate signalling in mammalian cells. Biochem J. 2000(349):385-402.

Rachner TD, Khosla S, Hofbauer LC. Osteoporosis: now and the future. The Lancet. 2011;377(9773):1276-87.

Ryu J, Kim HJ, Chang EJ, Huang H, Banno Y, Kim HH. Sphingosine 1-phosphate as a regulator of osteoclast differentiation and osteoclast-osteoblast coupling. EMBO J. Dec 13 2006;25(24):5840-51. Epub 2006/11/25.

Santa Cruz Biotechnology Inc. SphK1 (G-11): sc-365401 https://datasheets.scbt.com/sc-365401.pdf October 9, 2018

Schiefler C, Piontek G, Doescher J, Schuettler D, Mißlbeck M, Rudelius M, et al. Inhibition of SphK1 reduces radiation-induced migration and enhances sensitivity to cetuximab treatment by affecting the EGFR/SphK1 crosstalk. Oncotarget. 2014;5(20):9877-88.

Seref-Ferlengez Z, Kennedy OD, Schaffler MB. Bone microdamage, remodeling and bone fragility: how much damage is too much damage? Bonekey Rep. 2015;4:644. Epub 2015/04/08.

Shao JJ, Peng Y, Wang LM, Wang JK, Chen X. Activation of SphK1 by K6PC-5 Inhibits Oxygen-Glucose Deprivation/Reoxygenation-Induced Myocardial Cell Death. DNA Cell Biol. Nov 2015;34(11):669-76. Epub 2015/08/27.

Shiwaku Y, Neff L, Nagano K, Takeyama K, de Bruijn J, Dard M, et al. The Crosstalk between Osteoclasts and Osteoblasts Is Dependent upon the Composition and Structure of Biphasic Calcium Phosphates. PLoS One. 2015;10(7):e0132903. Epub 2015/07/21.

Song L, Xiong H, Li J, Liao W, Wang L, Wu J, et al. Sphingosine kinase-1 enhances resistance to apoptosis through activation of PI3K/Akt/NF-kappaB pathway in human non-small cell lung cancer. Clin Cancer Res. Apr 1 2011;17(7):1839-49. Epub 2011/02/18.

Spiegel S, Milstien S. Sphingosine-1-phosphate: an enigmatic signalling lipid. Nat Rev Mol Cell Biol. May 2003;4(5):397-407. Epub 2003/05/03.

Teti A. Mechanisms of osteoclast-dependent bone formation. Bonekey Rep. Dec 4 2013;2:449. Epub 2014/01/15.

Teti A, Econs MJ. Osteopetroses, emphasizing potential approaches to treatment. Bone. Sep 2017;102:50-9. Epub 2017/02/09.

Tolar J, Teitelbaum SL, Orchard PJ. Mechanisms of disease: Osteopetrosis. N Engl J Med. 12/30/2004 2004(351):2839-49.

Tortora GJ, Derrickson BH. Anatomie und Physiologie. Weinheim: Wiley-VCH-Verl.; 2008. XXVI, 1438 S. p.

Visekruna M, Wilson D, McKiernan FE. Severely suppressed bone turnover and atypical skeletal fragility. J Clin Endocrinol Metab. Aug 2008;93(8):2948-52. Epub 2008/06/05.

Vu TM, Ishizu AN, Foo JC, Toh XR, Zhang F, Whee DM, et al. Mfsd2b is essential for the sphingosine-1-phosphate export in erythrocytes and platelets. Nature. Oct 26 2017;550(7677):524-8. Epub 2017/10/19.

Xia P, Gamble JR, Wang L, Pitson SM, Moretti PAB, Wattenberg BW, et al. An oncogenic role of sphingosine kinase. Curr Biol. 11/17/2000 2000;10:1527-30.

10. Addendum

10.1 Figure Legends

10.2 Tables